I S O T O P E S H I F T I N C A D M I U M

- o - o -

A Thesis

Presented to the

Faculty of Graduate Studies

and Research of

The University of Manitoba

- x - x -

In Partial Fulfillment

of the Requirements for the Degree

Master of Science

- + - + -

by

Rubén Horacio Contreras

November 1968

---- # ----

c Rubén Horacio Contreras 1968

TABLE OF CONTENTS

TABLE OF CONTENTS

Chapter I

I N T R O D U C T I O N

The first observations made in the hfs of cadmium were due to Schüler and Bruck in 1929 and were published in Zeits. Phys. 56, 291, as is cited in "The Structure of Line Spectra"[38]. One of the authors of this book (Goudsmit, S.) found some misinterpretations in that paper, and published another one with his conclusions (Naturwiss. 17, 805, (1929)). Later Goudsmit and Bacher[17] used these values to apply the formulas that they found for the hfs splitting.

Fermi and Segrè[15] with data taken from Schüler and Keyston (Zeit. f. Phys. 71, 413, (1931)) pointed out that both odd isotopes, Cd^{111} and Cd^{113}, have I = ½, and the same splitting, indicating that the nuclear magnetic moments of both isotopes are equal. They mentioned the hfs splittings for the configurations 5s6s and 5s6p are both inverted and mainly due to the effect of the 5s electron.

They obtained the relation $\mu_{Bohr}/\mu = -3500$, with a large uncertainty because n_{eff} of the 5s orbit was not precisely known.

In Atomic Energy Levels[37] the summary given by Mack[34] is cited for cadmium II. This paper[34] contains a table of nuclear moments measured up to January 1950 and it is accompanied by a discussion on the subject. For cadmium a zero mechanical

moment in the even isotopes is reported in this paper (as it is the case with all even-even nuclei according to the present knowledge). For the odd isotopes a mechanical moment of ½ ℏ is reported using the data given by Schüler and Bruck in the paper mentioned above, and the magnetic moments for these odd isotopes are given as: $-0.59492 \pm 8 \times 10^{-5}$ n.m. for Cd^{111} and $-0.62238 \pm 8 \times 10^{-5}$ n.m. for Cd^{113}. These values for the magnetic moment come from the nuclear magnetic resonance experiment of Proctor and Yu[39]. No quadrupole moment is reported in any of the isotopes.

Goudsmit[18] in 1933 has used the data of Atomic Energy States[1] to calculate the g(I) factor for the different isotopes of cadmium. He has used the splitting factor with the Breit's and Racah's relativistic correction (see equations (41) and (42) of chapter II - a) for several elements. In this paper no mention is made to the Fermi and Segrè correction factor for s-electrons. Both papers[18],[15] were published in the same year of 1933. The formulas that Goudsmit has used are:

for s-electrons:

$$g(I) = \frac{3an_o^3 \times 1838}{8R\alpha^2 Z_i Z_o^2 K(\frac{1}{2}, Z_i)} \qquad (1)$$

where:

a is the hyperfine splitting factor for a single electron,

n_o and Z_o are the outer principal quantum number and

the outer effective nuclear charge,

Z_i is the inner effective nuclear charge,

α is the fine structure constant,

R is the Rydberg constant,

$K(\frac{1}{2},Z_i)$ is the relativistic correction given in equation (42) of chapter II - a (there it is called F_r) with $J = \frac{1}{2}$.

for non-s-electrons:

$$g(I) = \frac{aZ_i j(j+1)(1+\frac{1}{2})\lambda(1,Z_i)}{\Delta\nu\, l(l+1)\, K(j,Z_i)} \qquad (2)$$

where:

$\Delta\nu$ is the splitting for the ordinary spin doublets, and

$\lambda(1,Z_i)$ is a relativistic correction for $\Delta\nu$.

Goudsmit has calculated the same g(I) factor for both Cd^{111} and Cd^{113} and hence the same nuclear magnetic moment. His results are: $g(I) = -1.33$ and $\mu = -0.67$ n.m. though he noted that it is not certain whether Cd^{111}, Cd^{113} or both cause the observed hyperfine structure.

In 1933, Jones[24] investigated the Cd II spectrum in the region between 4200 and 8500 Å with Fabry-Perot etalons. Among the 14 lines he examined, only the line 8067 Å ($6^2S_{\frac{1}{2}} - 6^2P_{3/2}$) had any measurable structure. The line 8530 Å ($6^2S_{\frac{1}{2}} - 6^2P_{\frac{1}{2}}$) was faint and therefore was not completely analyzed. However, he

observed indications of the same structure as the one shown in 8067 Å. Jones found g(I) = - 1.25 for the odd isotopes Cd^{111} and Cd^{113}.

Proctor and Yu[39] in 1949 used a nuclear induction spectrometer to measure the magnetic moments of Sn^{115}, Cd^{111}, Cd^{113}, Pt^{195} and Hg^{199}. With samples of cadmium enriched to about 80 % in Cd^{111} and Cd^{113} they found a magnetic moment of - 0.5922 ± 0.0002 n.m. for Cd^{111} and - 0.6194 ± 0.0002 n.m. for Cd^{113}.

In the same year, 1949, Leland and Nier[32] working with a 60° mass spectrometer determined the relative isotope abundance in Zn and Cd. For Cd they reported the relative isotopic abundance shown in Table I.

TABLE I

Relative isotopic abundance in natural cadmium

Isotope	106	108	110	111	112	113	114	116
Relative abundance	1.215	0.875	12.39	12.75	24.07	12.26	28.86	7.58

This isotopic abundance is the one reported by Strominger et al.[46] in the 1958 Table of Isotopes.

In 1956 Kuhn and Ramsden[31] used different samples of

enriched isotopes to measure the hfs of 4416 Å ($4d^{10}5p\ ^2P_{3/2}$ - $4d^9 5s^2\ ^2D_{5/2}$) which is a transition involving two s-electrons and therefore shows a large isotope shift. This transition has been studied before by several authors (see references in Kuhn and Ramsden paper). Kuhn and Ramsden used a single Fabry-Perot interferometer but for higher resolution for some observations used a double one. The light source was a hollow cathode cooled with liquid hydrogen. They found that the shifts between succesive even isotopes decrease with increasing neutron number in an irregular manner. With these measurements they found that the odd-even staggering is pronounced.

In 1957 Sutherland[47] has measured the hfs of the resonance lines 2144 Å ($5s\ ^2S_{1/2}$ - $5p\ ^2P_{3/2}$) and 2265 Å ($5s\ ^2S_{1/2}$ - $5p\ ^2P_{1/2}$) in Cd II in order to obtain the magnetic hyperfine structure of the 5s level and to check the validity of the Fermi-Segrè factor calculated by the method of Crawford and Schawlow[11] (see equations (39), (40) and (41) of chapter II - a). The light source was a hollow cathode cooled with liquid nitrogen. The high resolution was provided by a Fabry-Perot interferometer crossed with the same Hilger Spectrograph used in the present work. He recorded each of the lines with two different spacers, namely, 0.518 cm and 1.255 cm. With the 0.518 cm spacer, both lines showed one strong and broad component, ascribed to the even

isotopes and a fainter one, ascribed to the a component of the odd isotopes (see fig. I - 1). With the spacer 1.255 cm both lines showed three components, a broad and intense one, ascribed as before to the even isotopes, and two faint components considered to be the a component and the non-resolved b and c components of the odd isotopes (see figs. I - 4 and I - 5). With these assumptions, a fairly good agreement was found between the calculated magnetic moment using the Fermi-Segrè factor and the values of the moment found by proctor and Yu[39]. However, the isotope shift between the center of gravity of the odd isotopes and that of the even isotopes for the two transitions were not consistent.

In 1959, Kelly and Tomchuk[26], using the atomic beam light source used in the present work, measured the isotope shifts in the line 3261 Å ($5s^2\ ^1S_0 - 5s5p\ ^3P_1$) of cadmium I. A Fabry-Perot was used to obtain the high resolution. They found agreement between their measurement of isotope shifts with those previously reported in other cadmium lines.

In 1961, the same authors[27] using the same method, measured the isotope shifts in the line 2288 Å ($5s^2\ ^1S_0 - 5s5p\ ^1P_1$). Comparing the shifts found from the two lines they concluded that the specific mass effect is small (see Tomchuk's PhD thesis, University of Manitoba[50]).

I - a) The present problem

Kopfermann[29] in page 173 points out that the $6s^2$ configuration

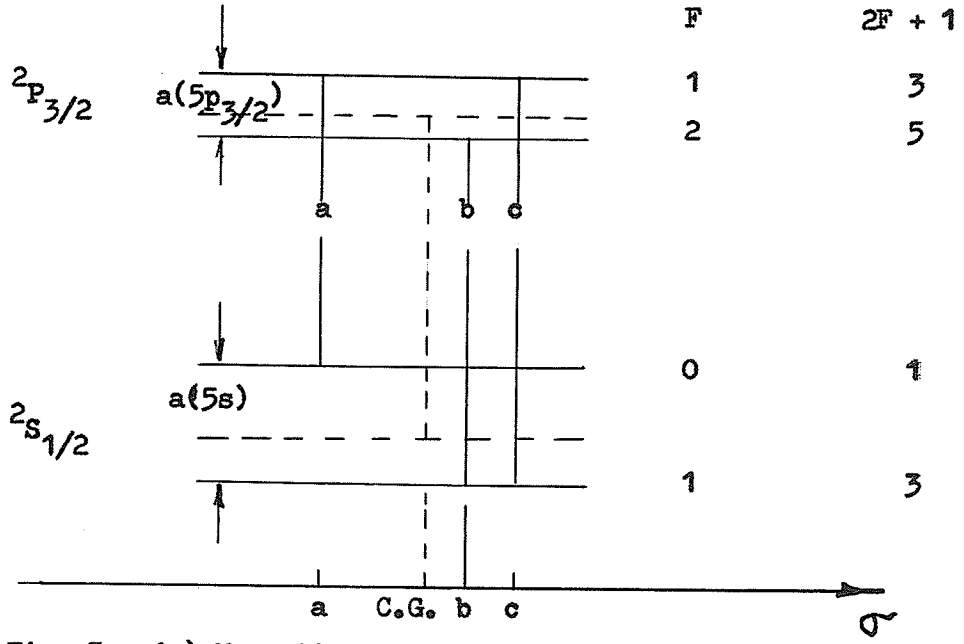

Fig. I - 1a) Magnetic structure of the odd isotopes in the 2144 Å line, showing the relative intensities and positions of their components (not to scale).

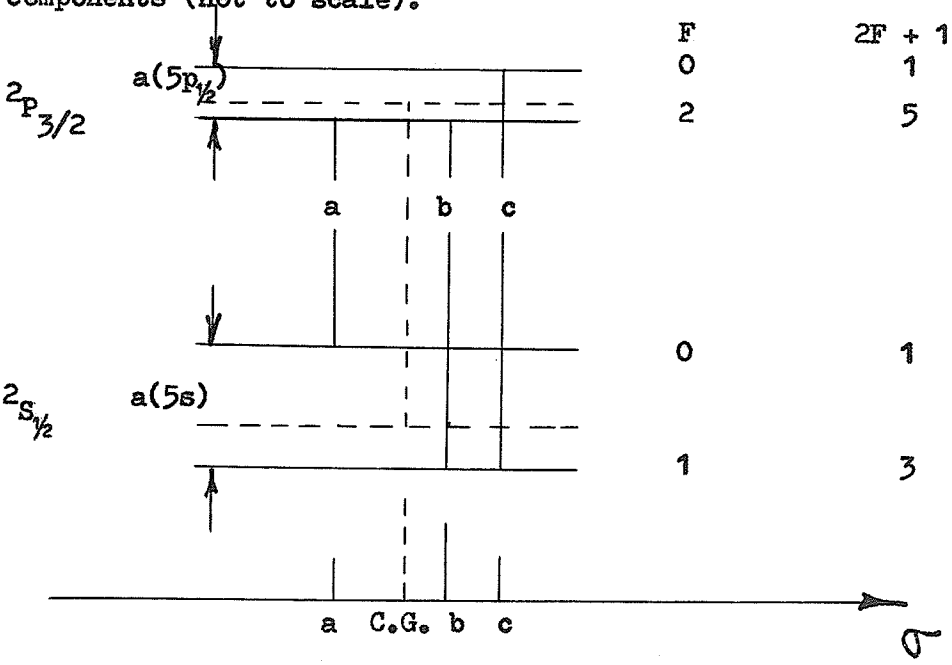

Fig. I - 1b) Magnetic structure of the odd isotopes in the 2265 Å line, showing the relative intensities and positions of their components (not to scale).

in Hg I has an isotope shift which is 1.6 times that of the 6s configuration in Hg II. As these configurations are similar to those in Cd I and Cd II it should be expected that a similar relation between the isotope shifts in the 5s configuration of these two atoms can be found. Then, using the results obtained by Kelly and Tomchuk[26] an approximate estimation may be made for the isotope shifts in the 5s level of Cd II. The isotope shifts in Cd I 3261 Å are shown in fig. I - 2. While in fig. I - 3 the expected isotope shifts for Cd 2265 Å are given. The expected Cd II shifts are found by multiplying those for Cd I 3261 Å by 1.6. The center of gravity of the odd isotopes in Cd 3261 Å is found from fig. I - 2, to be at 11.6 mk on high frequency side of the center of gravity of the even isotopes. This yields for Cd 2265 Å a separation between the center of gravity of odd and even isotopes of approximately 19 mk, with the odds' center of gravity on high frequency side of evens'. (*)

If the data given by Sutherland[47] are re-interpreted, considering that he took a wrong interference order in his measurements with the spacer 1.255 cm, the validity of the Fermi-Segrè factor can be verified within the same limits, and consistent values of the isotope shifts between the center of gravity of the odds and evens is found for the two lines examined

(*): For these ideas the author is indebted to Dr. E. Tomchuk.

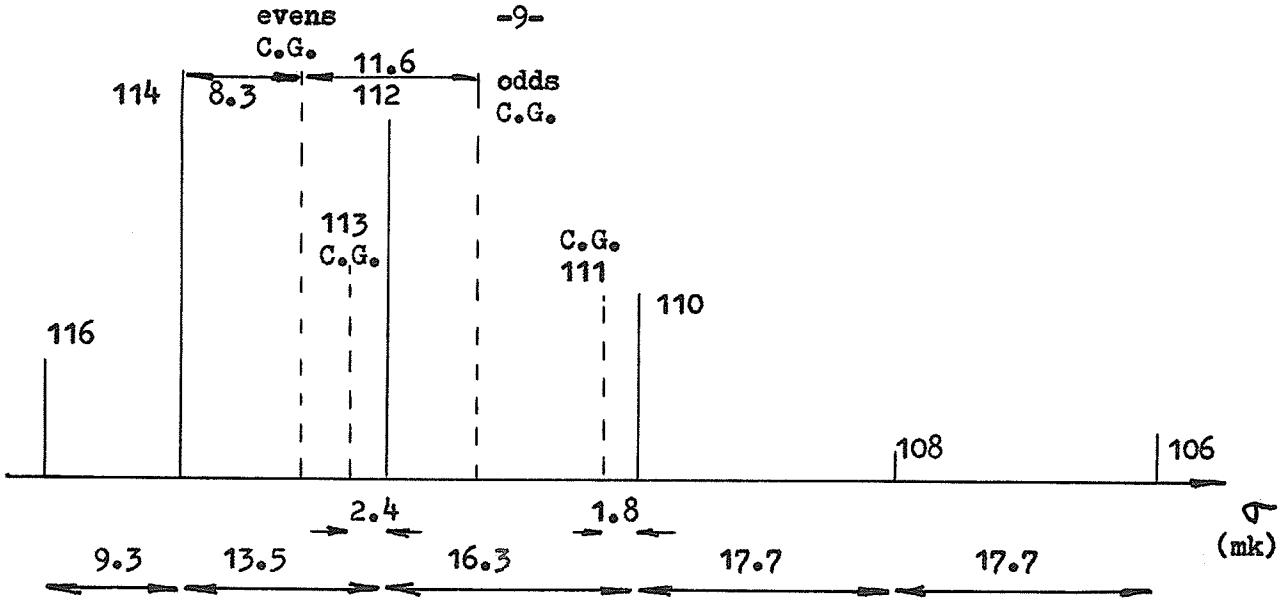

Fig. I - 2) Isotope shifts in Cd I 3261 Å. Each component is labelled with its mass number. The relative intensities shown are estimated from the relative isotope abundance. The relative intensities as well as the isotope shifts are shown to scale.

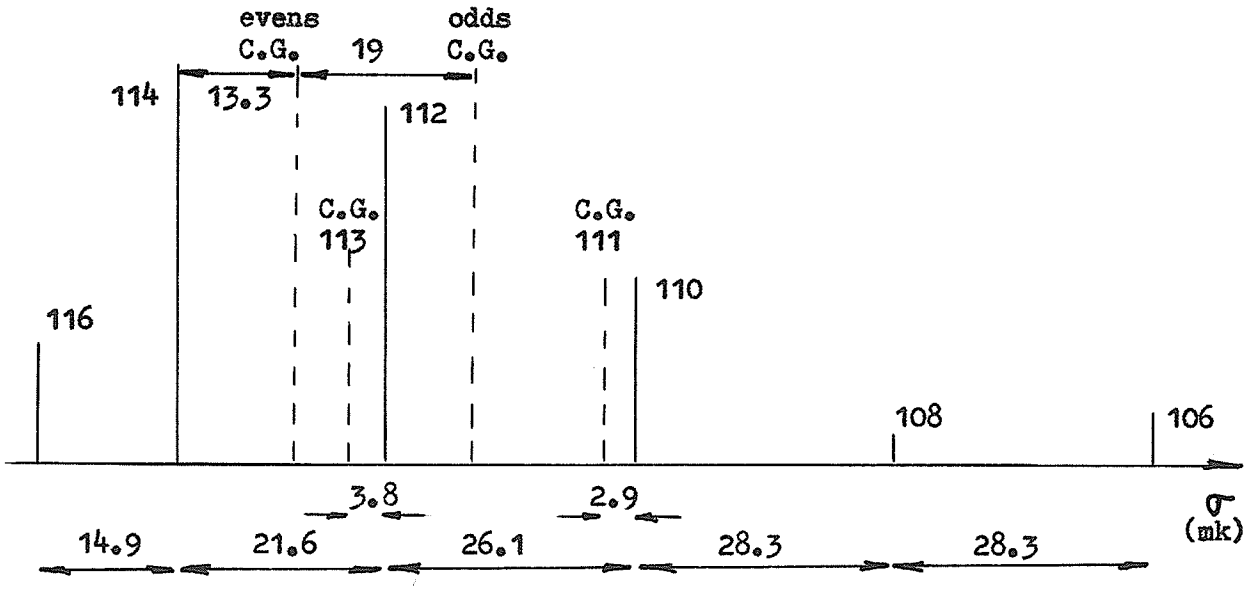

Fig. I - 3) Isotope shift in Cd II 2265 Å as calculated from fig. I - 2 multiplying the isotope shifts shown there times 1.6. The relative intensities are estimated in the same way as in fig. I - 2. Both the relative intensities and the isotope shifts are shown to scale.

by Sutherland. These are 23 mk for 2144 Å and 19 mk for 2265 Å. Moreover, these new values compare favorably with those obtained when the isotope shifts in 3261 Å of Cd I are multiplied by 1.6 (see figs. I - 4 and I - 5).

The line width in the source used by Sutherland made a direct determination of the isotope shift between the even isotopes impossible and supplied only partial information on the odd-even shifts. The aim of this work is to measure the isotope shifts between the naturally ocurring cadmium isotopes directly and to use lines in the Cd II spectrum. The Cd II ion has one valence electron while Cd I has two. For this reason theoretical formula can be more directly applied to Cd II data. As well, an attempt is made to resolve the discrepancy in the relative isotope shifts observed in 3261 Å by Kelly and Tomchuk[26] and those observed by Kuhn and Ramsden[31] in 4416 Å.

The magnetic hfs splitting of the 2265 Å, according to the new interpretation of Sutherland's results, is given in fig. I - 6. It should be kept in mind that each component is produced by an overlapping of components due to each of the odd isotopes as the resolution was not high enough to resolve them. In fig. I - 7, the magnetic hfs splitting of Cd II 2144 Å, is given according to the re-interpretation of Sutherland's results. In this case also the resolution was not high enough to resolve the components due to the two different isotopes of mass numbers 113 and 111.

As the magnetic moment of Cd^{113} is not the same as the one in Cd^{111} the center of gravity of each magnetic component does not lie midway between the component produced by Cd^{111} and that of Cd^{113}.

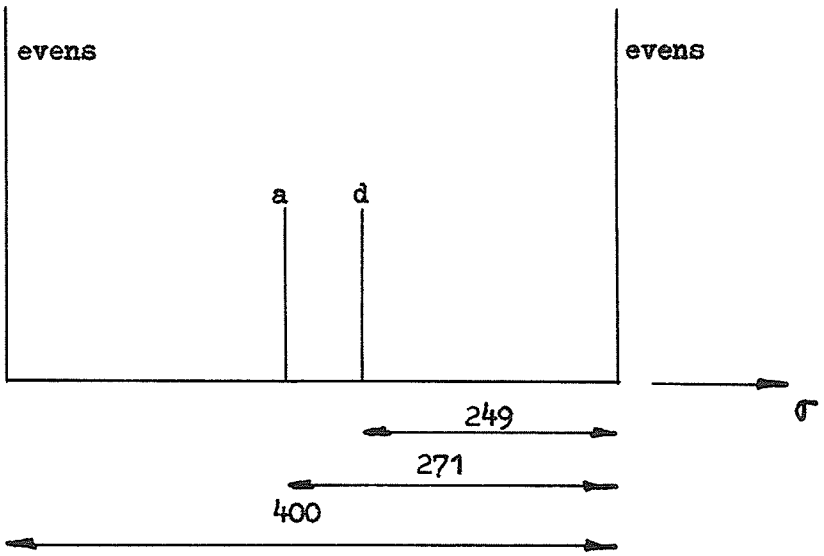

Fig. I - 4a) Sutherland's interpretation of his data. d: center of gravity of the non-resolved b and c components (see fig. I - 1). This is a schematic drawing of the pattern obtained in (47) with the 1.255 cm spacer in the line 2144 Å. The interorder is 400 mk. All separations are given in mk.

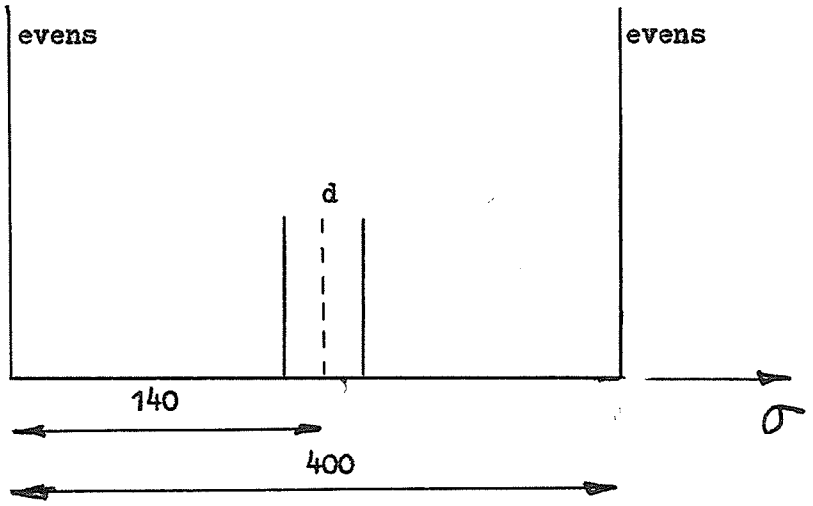

Fig. I - 4b) The same schematic drawing shown in fig. I - 4a, but according to the new interpretation. Instead of being components a and d, the only ring assumed to appear is the non-resolved d. (Actually there are four components in it.) According to this assumption it is found: a(5s) = 479 mk. The distance between the centers of gravity of odds and evens is 23 mk.

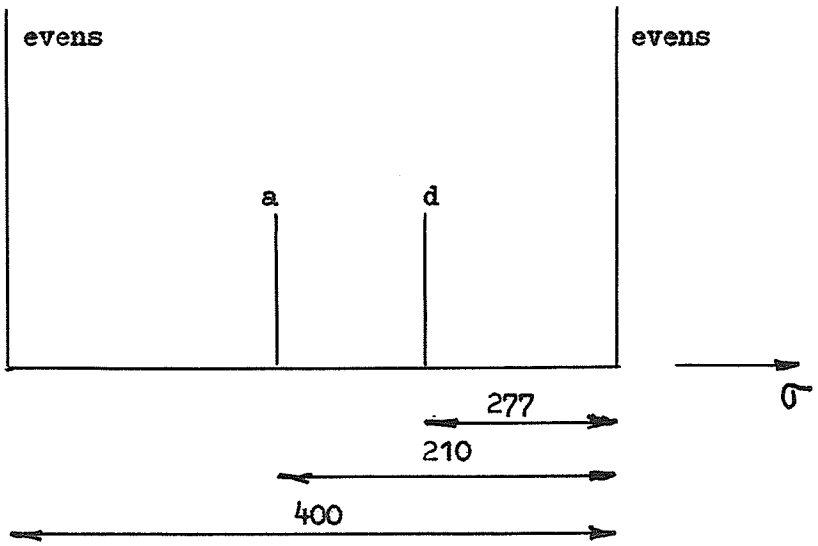

Fig. I - 5a) Schematic drawing of the pattern obtained by Sutherland[47] with the 1.255 cm spacer for the line 2265 Å and his interpretation. The interorder is 400 mk. d stands for the center of gravity of the assumed non-resolved b and c components. All separations are given in mk units.

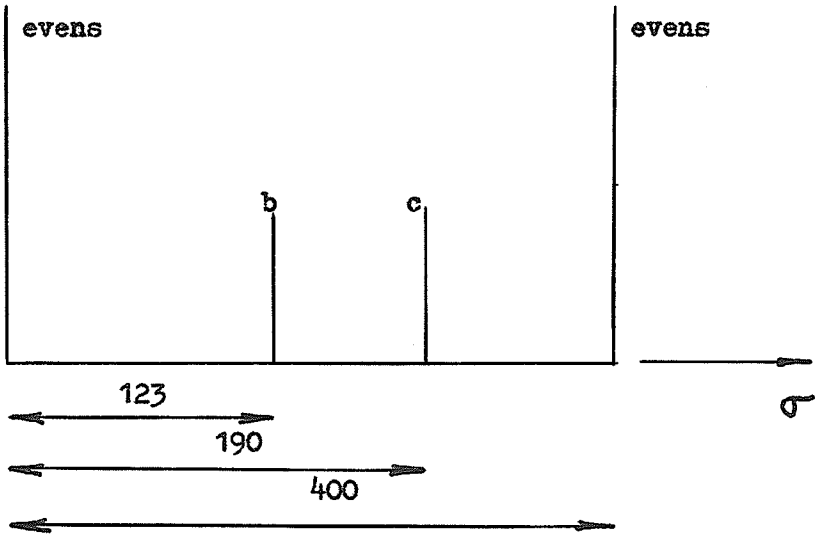

Fig. I - 5a) The same schematic drawing shown in part a of this figure but according to the new interpretation. Instead of being a and d components observed in this pattern, b and c components are resolved and are the only ones which appear. The a component is masked with the broad fringe produced by the even components. b and c components belong to the same order.

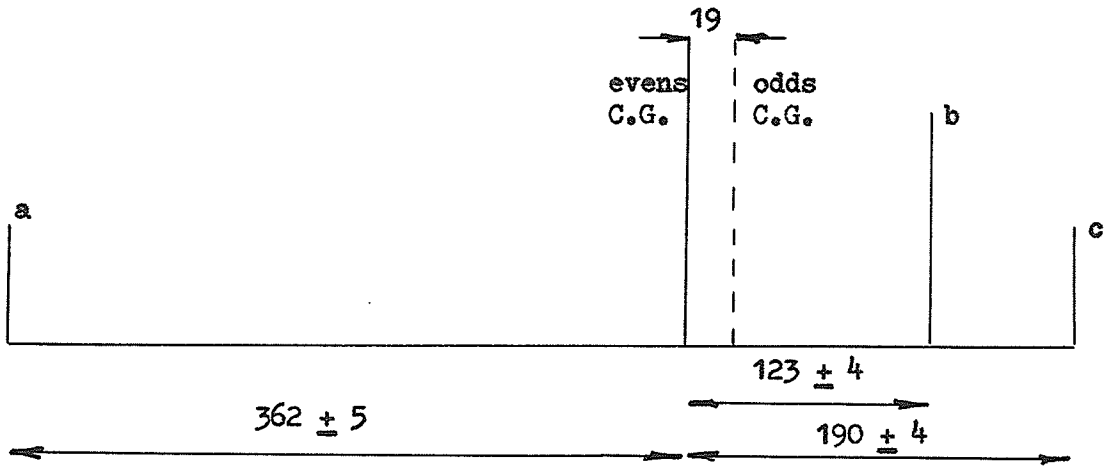

Fig. I - 6) Magnetic hfs splitting in Cd II 2265 Å, according to the new interpretation of Sutherland's data. The distances are given in mk. The errors are taken from Sutherland's[47] interpretation. The resolution was not high enough to resolve the components due to the odd isotopes 111 and 113.

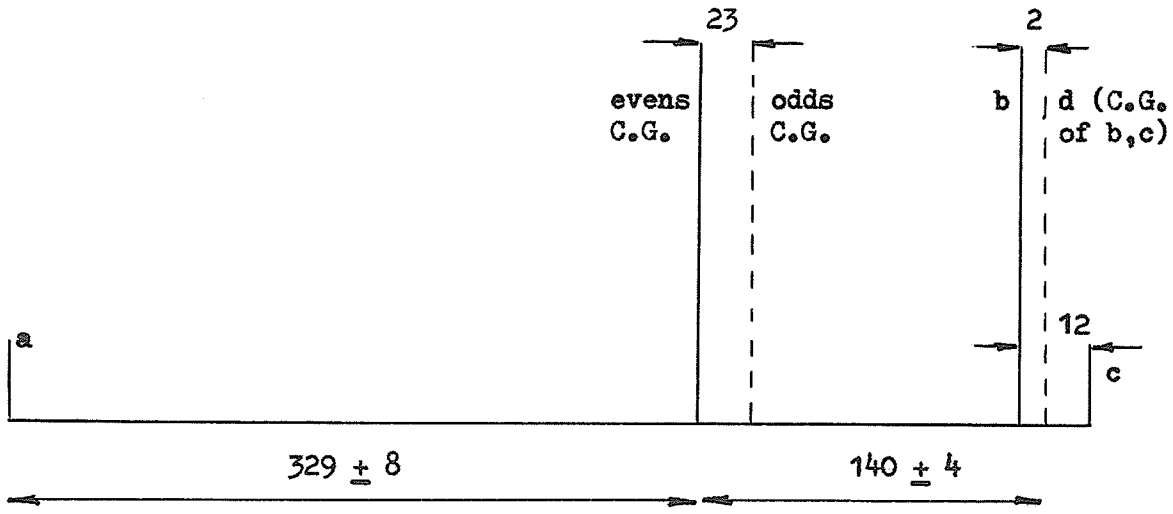

Fig. I - 7) Magnetic hfs splitting in Cd II 2144 Å, according to the re-interpretation of Sutherland's[47] data. The distances are given in mk. The errors as well as the distances between d and b, and d and c, are taken from Sutherland's calculations. Again the resolution was not high enough to resolve the contributions due to the isotopes 113 and 111.

Chapter II

ELEMENTS OF THE THEORY OF HFS

When lines which arise from individual multiplet are examined with a high resolution spectrograph, it is found that many lines in the spectra of atoms are split into a number of components generally lying very close together. This splitting is called hyperfine structure, which is abbreviated hfs. There are two kinds of phenomena included in hfs, a) an electromagnetic interaction between the electron charge density and the nuclear charge density, and b) the so-called isotope structure or isotope shift.

II - a - 1) Electromagnetic Interaction

The electromagnetic interaction between the electron and nuclear charge density is considered in a number of books and papers. The ideas presented here are mainly taken from the approaches given by Kopfermann[29], Kelly[25], Casimir[7], White[54], Goudsmit[16] and Herzberg[19].

Using the laws of classical electrodynamics[22] the electromagnetic interaction energy between two current and charge densities may be written as:

$$E_{int.} = -\left(\iint \frac{\rho_1(\bar{r}_1)\,\rho_2(\bar{r}_2)\,dv_1 dv_2}{r_{12}} \right. \quad +$$

$$+ \iint \frac{\bar{j}_1(\bar{r}_1) \cdot \bar{j}_2(\bar{r}_2)\ dv_1 dv_2}{r_{12}} \quad) \qquad (1)$$

where:

$\rho_1(\bar{r}_1)$ is the charge density of the electrons at $\bar{r}_1$ position,

$\rho_2(\bar{r}_2)$ is the charge density of the nucleus at $\bar{r}_2$ position,

$\bar{j}_1(\bar{r}_1)$ is the current density of the electrons at $\bar{r}_1$ position,

$\bar{j}_2(\bar{r}_2)$ is the current density of the nucleus at $\bar{r}_2$ position, and

$$r_{12} = \left| \bar{r}_1 - \bar{r}_2 \right|$$

This in turn may be written as:

$$E_{int} = - \int \rho_2(\bar{r}_2)\ \phi(\bar{r}_2)\ dv_2 \quad - \frac{1}{c} \int \bar{A}(\bar{r}_1) \cdot \bar{j}_1(\bar{r}_1)\ dv_1 \qquad (2)$$

where:

$$\phi(\bar{r}_2) = \int \frac{\rho_1(\bar{r}_1)\ dv_1}{r_{12}} \qquad (3)$$

is the electrostatic potential produced by the orbital electrons at $\bar{r}_2$, and

$$\bar{A}(\bar{r}_1) = \frac{1}{c} \int \frac{\bar{j}_2(\bar{r}_2)\, dv_2}{r_{12}} \qquad (4)$$

is the nuclear vector potential produced at $\bar{r}_1$.

The origin of co-ordinates is taken at the center of mass of both the nuclear charge distribution and the orbital electron density. For electrons whose charge density is zero at the center of mass, equation (3) may be expanded according to Jackson[32], page 101:

$$\phi(\bar{r}_2) = \phi(0) - \bar{r}_2 \cdot \bar{F}(0) - \frac{1}{6} \sum_{i,j} (3x_i x_j - r_2^2 \delta_{ij}) \frac{\partial F_j(0)}{\partial x_i} + \cdots \qquad (5)$$

where x_i, x_j are the components of $\bar{r}_2$,

and $\bar{F} = - \bar{\nabla} \phi$

Outside the nucleus equation (4) may be expanded according to Jackson[22], page 145:

$$\bar{A}(\bar{r}_1) = \frac{\bar{\mu}_I \times \bar{r}_1}{r_1^3} + \cdots, \qquad (6)$$

where

$$\bar{\mu}_I = \frac{1}{2c} \int \bar{r}_2 \times \bar{j}_2(\bar{r}_2)\, dv_2$$

which is defined as the magnetic moment of the nuclear current distribution $\bar{j}_2(\bar{r}_2)$.

Carring equations (5) and (6) into equation (2):

$$E_{int} = -\int \rho_2(\bar{r}_2)\phi(0)\, dv_2 + \bar{F}(0)\cdot\int \bar{r}_2 \rho_2(\bar{r}_2)\, dv_2 + \sum_{i,j} \frac{1}{6}\frac{\partial F_j(0)}{\partial x_i}\int (3x_i x_j - r_2^2 \delta_{ij})\, dv_2 - \int \frac{(\bar{\mu}_I \times \bar{r}_1)\cdot \bar{j}_1(\bar{r}_1)}{r_1^3}\, dv_1 \qquad (7)$$

Quantum mechanically the system formed by the nucleus, considered as a point, and the electrons, and described by the product of the eigenfunctions of the electrons times the eigenfunctions of the nucleus will suffer a perturbation whose Hamiltonian is given by the difference between equation (7) and the interaction energy assuming a point nucleus, namely:

$$H' = E_{int} - \sum_i \frac{-Ze^2}{r_i} \qquad (8)$$

where Ze is the nuclear charge, and the summation is extended over all electrons.

Obviously the first term in equation (7) will cancel with the second one in equation (8). Besides in equation (7):

$$\int \bar{r}_2 \, \rho_2(\bar{r}_2) \, dv_2 = \bar{p} \qquad (9)$$

where $\bar{p}$ is the electric dipole moment of the nucleus. Here it is important to recall that no nuclear electric dipole has ever been observed. In fact, an electric dipole moment must have an expectation value of zero for any quantum mechanical system with a definite parity. Then the second term in equation (7) may be neglected.

In the last term of equation (7) the cross and dot products may be interchanged, giving:

$$\int \frac{(\bar{\mu}_I \times \bar{r}_1) \cdot \bar{j}(\bar{r}_1) \, dv_1}{r_1^3} = \int \frac{\bar{\mu}_I \cdot (\bar{r}_1 \times \bar{j}_1(\bar{r}_1)) \, dv_1}{r_1^3} \qquad (10)$$

But:

$$\int \frac{\bar{r}_1 \times \bar{j}_1(\bar{r}_1)}{r_1^3} \, dv_1 = \bar{H}_o$$: magnetic field caused by

$\bar{j}_1(\bar{r}_1)$ at the origin.

Using equations (9), (10) and (11) in (8):

$$H' = - \bar{\mu}_I \cdot \bar{H}_o + \sum_{ij} \frac{1}{6} \frac{\partial F_j(0)}{\partial x_i} \quad (3x_i x_j - r_2^2 \delta_{ij}) \rho_2 \, dv_2 . \qquad (12)$$

The nuclear magnetic moment may be written in the form:

$$\bar{\mu}_I = \frac{e\hbar}{2Mc} \, g_I \, \bar{I} \qquad (13)$$

where:

M is the mass of the proton,

g_I is the numerical nuclear g factor, and

$\bar{I}$ is the nuclear spin.

The magnetic field $\bar{H}_o$ may be written as:

$$\bar{H}_o = k\bar{J}$$

where: $\bar{J}$ is the total electronic angular momentum, and

k is a constant which may be calculated computing the expectation value of H_z when m = J

$$k = \frac{1}{J}(n,J,m = J \quad \left| H_Z \right| \quad n,J,m = J) = \frac{1}{J} \quad \bar{H}(\bar{0}) . \qquad (14)$$

With the help of equations (13) and (14) the first term of equation (12) may be written:

$$H' = H'_m + H'_e = - \frac{e\hbar}{2McJ} \, g_I \, \bar{H}(\bar{0}) \, (\bar{I}.\bar{J}) + H'_e \qquad (15)$$

where: H'_m and H'_e stand for the magnetic and the electrostatic interaction, respectively.

According to the definition of the operator $\bar{F} = \bar{I} + \bar{J}$ the following relation holds:

$$\bar{I}.\bar{J} = \tfrac{1}{2}(\bar{F}^2 - \bar{I}^2 - \bar{J}^2),$$

where it is apparent that when a representation in which $\bar{F}^2$, $\bar{I}^2$ and $\bar{J}^2$ are diagonal is used, the operator H'_m in equation (15) will also be diagonal. Then it is possible to replace in the latter equation the operators for their eigenvalues. After doing that equation (15) will take the form:

$$H' = -\frac{e\hbar g_I}{2Mc2J}\,\bar{H}(\bar{0})\left[F(F+1) - I(I+1) - J(J+1)\right] + H'_e =$$

$$= \tfrac{1}{2}\,AC + H'_e \qquad (16)$$

where:

$$A = -\frac{e\hbar g_I}{2McJ}\,\bar{H}(\bar{0}) = \frac{\mu_I\,\bar{H}(\bar{0})}{IJ}$$

and $C = F(F+1) - I(I+1) - J(J+1)$.

At the nucleus the divergence of the electric field $\bar{F}(\bar{r})$ is zero:

$$\bar{\nabla}.\bar{F}(\bar{r}) = 0 \qquad (17)$$

Since $\emptyset$ has cylindrical symmetry about the z-axis,

equation (17) yields:

$$\frac{\partial F_z}{\partial z} = -2\frac{\partial F_y}{\partial y} = -2\frac{\partial F_x}{\partial x} \qquad (17)a$$

and it is possible to give a simpler expression to H'_e in equation (12) since grad $\bar{\bar{F}}$ may be refered to its principal axis, i.e.:

$$\frac{\partial F_j}{\partial x_i} = 0 \text{ if } i \neq j. \quad \text{if } i = j \text{ then equation (17)a holds.}$$

H'_e may be written as:

$$H'_e = \frac{1}{6} e \left\{ \frac{\partial F_x}{\partial x} \int (3x^2 - r_2^2) \rho_2 \, dv_2 + \frac{\partial F_y}{\partial y} \int (3y^2 - r_2^2) \rho_2 dv_2 + \right.$$

$$\left. + \frac{\partial F_z}{\partial z} \int (3z^2 - r_2^2) \rho_2 dv_2 \right\} = \frac{1}{6} e \left\{ -\tfrac{1}{2} \frac{\partial F_z}{\partial z} \int (3x^2 - r_2^2) \rho_2 \, dv_2 - \right.$$

$$- \tfrac{1}{2} \frac{\partial F_z}{\partial z} \int (3y^2 - r_2^2) \rho_2 \, dv_2 + \frac{\partial F_z}{\partial z} \int (3z^2 - r_2^2) \rho_2 \, dv_2 =$$

$$= H'_e = \tfrac{1}{4} \frac{\partial F_z(0)}{\partial z} e \int (3z^2 - r_2^2) \rho_2 \, dv_2 \qquad (18)$$

where this expression is refered to the principal axis of the tensor grad $\bar{\bar{F}}(\bar{r})$.

The integral in equation (18) is known as the quadrupole moment of the nucleus:

$$eQ' = e \int (3z - r_2^2) \rho_2 \, dv_2 \qquad (19)$$

To write it in terms of the symmetry axis of the nucleus a change of co-ordinates must be made. If ϕ is the angle between the symmetry axis of the field and the symmetry axis of the nucleus, then:

$$eQ' = eQ \cdot \tfrac{1}{2}(3 \cos^2\phi - 1) \qquad (20)$$

with eQ the quadrupole moment of the nucleus refered to its principal axis.

From equations (18), (19) and (20):

$$H'_e = \tfrac{1}{4} \frac{\partial F_z(0)}{\partial z} \, eQ \cdot \tfrac{1}{2}(3\cos^2\phi - 1) \qquad (21)$$

This classical interaction energy is expected to be the same as the quantum mechanical result for large quantum numbers. As before, cos ϕ may be replaced by:

$$\cos\phi = \frac{\bar{F}^2 - \bar{I}^2 - \bar{J}^2}{2\bar{I}^2\bar{J}^2} = \frac{F(F+1) - I(I+1) - J(J+1)}{2I(I+1)J(J+1)}.$$

When it is put into equation (21), for large quantum numbers

the result is the same as the quantum mechanical expression given by Casimir[7]:

$$H'_e = \frac{eQ}{4} \cdot \frac{\partial \overline{F_z(0)}}{\partial z} \cdot \frac{3/2 \cdot C(C+1) - 2I(I+1)J(J+1)}{I(2I-1)J(2J-1)} . \qquad (22)$$

where:

$$C = F(F+1) - I(I+1) - J(J+1).$$

It is common to write:

$$H' = \tfrac{1}{2} AC + \tfrac{1}{4} B \frac{\frac{3}{2} C(C+1) - 2I(I+1)J(J+1)}{I(2I-1)J(2J-1)} . \qquad (23)$$

This additional energy H' will produce a shift in the atomic energy levels which in turn will produce shifts in the lines of the spectra. To find the total energy that a given multiplet level will have including the hfs (equation (23)), it is necessary to add to the energy E_J of the multiplet level, the quantity H' which depends on the quantum number F. For fixed J and I the quantum number F takes the values:

$$F = I + J, \quad I + J - 1, \quad \ldots\ldots \quad |I - J| .$$

Thus a multiplet level characterized by a J value is split into $2J + 1$ states if $I \geq J$, or into $2I + 1$ states if $J \geq I$. The center of gravity of the hfs states is at the same position in the energy level diagram as the level when nuclear effects

are neglected (see fig. II - 1), provided the interaction energies between $\bar{S}$ and $\bar{I}$, and $\bar{L}$ and $\bar{I}$ are small compared with that between $\bar{S}$ and $\bar{L}$, in the Russell-Saunders coupling case; or the interaction energy with $\bar{I}$ is small compared with any other interaction involved when the coupling does not follow the L-S scheme. In general the splittings due to the magnetic and electrostatic hfs are much smaller than those of the fine structure splittings, and the assumptions concerning the $\bar{F}$ vector are justified to a greater extent than the corresponding assumptions made in the Russell-Saunders approximation for atomic fine structure.

When the interaction energy of $\bar{J}$ with $\bar{I}$ is weak compared to the interaction between the vectors which add up to give $\bar{J}$, a classical picture shows that there is a definite intensity rule among the components of a hfs multiplet. The coupling between the nuclear spin and the electronic system is so weak that it does not change the energy radiated in the line, but distributes it over the hfs components.

In many cases the intensity ratios may be determined using the sum rule originally given by Ornstein, Burger and Dorgelo (see reference in Atomic Spectra[30]) for fine structure multiplets: i) the sum of the intensities of all lines of a hfs multiplet which begin from a common initial state characterized by F, is proportional to its quantum weight $2F + 1$; ii) The sum of the intensities of all lines of a hfs multiplet which end

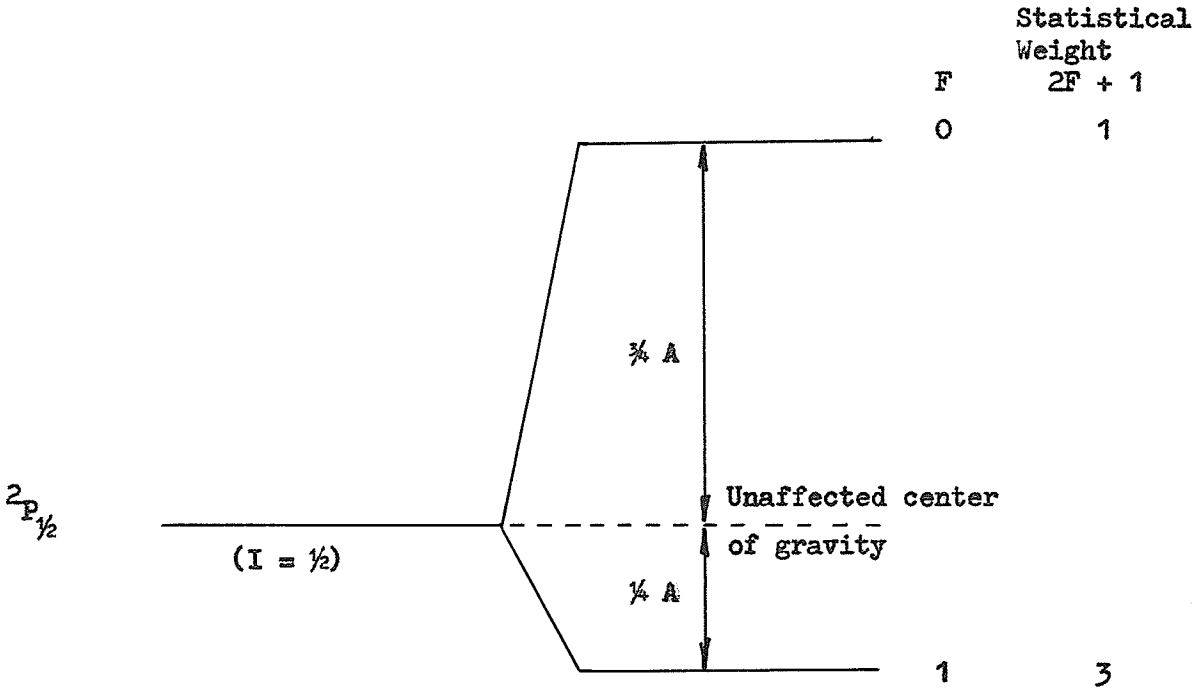

Fig. II - 1) Magnetic splitting in the $^2P_{½}$ level of Cd II. As the nuclear magnetic moment in Cd II is negative, the hfs levels present an inverted sequence, which means that the level with the largest F lies lowest. The electric quadrupole interaction energy vanishes identically since J = ½ and I = ½.

on a common final state characterized by F', is proportional to its quantum weight 2F' + 1. When both levels involved in a transition are split into hfs multiplets the sum rule as given above is not enough to determine the relative intensities of the components. In this case Kronig and Russell (see references in Atomic Spectra[30]) have derived formulas whose results are tabulated for the lines in a fine structure multiplet. To use them in the hfs multiplets, as before, the following substitution must be made: L ⟶ J, S ⟶ I and J ⟶ F. Examples of the application of the Burger and Dorgelo's sum rule are given in Atoms, Molecules and Quanta[42], and in the Theory of Atomic Spectra[8].

When the electric quadrupole interaction may be neglected, the splitting due to the magnetic interaction alone, follows the interval rule, established by Landé in fine structure, with the suitable change in symbols shown above. States differing in F values by unity are adjacent, and remembering the expression for C given in equation (22) it is apparent that the distance between them is AF, where F is the larger of the F's characterizing both states.

II - a - 2) The problem of determining the A constant in equation (23)

As it was pointed out before,

$$A = \frac{\mu_I \bar{H}(0)}{IJ}$$

To know A it is necessary to calculate $\bar{H}(0) = (n,J,m=J \left| H_z \right| n,J,m=J)$

The magnetic field produced at the nucleus by the orbital electrons when there is only one valence electron, may be thought of as produced by $\bar{L}$ and by $\bar{S}$:

$$\bar{H} = \bar{H}_L + \bar{H}_S$$

If classical arguments are used:

$$\bar{H}_L = - \frac{e(\bar{r} \times \bar{v})}{cr^3} = - \frac{e}{mcr^3} \cdot \bar{L}$$

$$H_S = \frac{3(\bar{r} \cdot \bar{\mu}_s)\bar{r}}{r^5} - \frac{\bar{\mu}_s}{r^3}$$

With these expressions for $\bar{H}$, it may be shown (see for example Hindmarsh[20] and Pauling and Goudsmit[38]) that:

$$\bar{H}(0) = \frac{2\mu_N \mu_B \, l(l+1)}{\hbar \, (j+1)} \cdot \left(\frac{\bar{1}}{r^3}\right) \qquad (24)$$

where:

μ_B is the Bohr magneton $= \frac{e\hbar}{2mc}$

and μ_N is the nuclear magneton = $\frac{e\hbar}{2Mc}$.

Using equation (24) in equation (16):

$$H'_m = \frac{2\mu_I\mu_S\, l(l+1)C}{2j(j+1)} \cdot \overline{\left(\frac{1}{r^3}\right)} \qquad (25)$$

Then:

$$a_j = \frac{2\mu_I\mu_S\, l(l+1)}{Ij(j+1)} \cdot \overline{\left(\frac{1}{r^3}\right)} \qquad (26)$$

It is common to designate the A values for one-valence-electron atoms with small a.

Quantitative estimations of E_{int} can be made provided g_I, which gives the value of the magnetic dipole moment of the nucleus, is known, and $\overline{r^{-3}}$ can be evaluated. For a hydrogen-like atom (see Davydov[12]) $\overline{r^{-3}}$ is given by:

$$\overline{\left(\frac{1}{r^3}\right)} = \frac{Z^3}{a_o^3 n^3 (l+1)(l+\tfrac{1}{2})l} \qquad (27)$$

where a_o is the radius of the first orbit in Bohr's atom and the other symbols stand for the meaning shown before.

Equation (27) provides an a_j value of:

$$a_j = \frac{2\mu_I \mu_S Z^3}{a_o^3 n^3 \, j(j+1)(l+\tfrac{1}{2})} \qquad (28)$$

When the valence electron occupies an s state, $l = 0$ and problems arise in $\overline{r^{-3}}$ as well as in $\overline{H(0)}$ as given by equation (24). However, according to more precise calculations (see Fermi and Segre[15] and Kopfermann[29]) it can be shown that to a first approximation it is justified to put simply $l = 0$ in equation (28) which, after that substitution and putting $j = \tfrac{1}{2}$ becomes:

$$a_o = \frac{16\mu_I \mu_S Z^3}{3a_o^3 n^3} = \frac{16\pi\mu_I \mu_S}{3} \cdot \psi_S^2(0) \qquad (29)$$

where $\psi_S^2(0) = \frac{Z^3}{\pi a_o^3 n^3}$ is the square of the Schrödinger function when $r = 0$, for s-electrons.

If instead of having a hydrogen-like atom one has an atom with only one electron out of closed shells (alkali-like configuration) the problem may be considered in a similar fashion applying the idea of penetrating orbits and making use of the correspondence principle (see for example White[54]). The motion of the valence electron in one of such orbits may be idealized by assuming that its orbit can be divided in two portions: the first one, where the valence electron is outside the electron core, and

the second one where the valence electron is inside the electron core. In this simple approximation the electrostatic potential seen by the electron out of closed shells is:

$$\phi(r) = Ze/r \qquad \text{if} \quad r < r_o$$

$$\phi(r) = Z_o e/r \qquad \text{if} \quad r > r_o$$

where r_o stands for the radius of the electron core (a quantity which cannot be well defined). Then in the two regions the wave function is hydrogen-like. In the outer region it has an effective quantum number n* instead of the actual one. Equation (24) still holds and now the problem consists in computing $\overline{r^{-3}}$. Using this approximation and equation (27) one has:

$$\overline{\left(\frac{1}{r^3}\right)}_2 = \frac{Z^3}{a_o^3 n^3 l(l+\tfrac{1}{2})(l+1)} \qquad \text{if} \quad r < r_o$$

$$\overline{\left(\frac{1}{r^3}\right)}_1 = \frac{Z_o^3}{a_o^3 n^{*3} l(l+1)(l+\tfrac{1}{2})} \qquad \text{if} \quad r > r_o \qquad (30)$$

The overall average may be found by weighing the contributions of the outer and inner portions in proportion to the transit times

t_1(for $r > r_o$) and t_2 (for $r < r_o$). The times t_1 and t_2 can be calculated assuming that the electron orbit is approximately a complete ellipse in any of the two portions. Therefore the time computed according to the Bohr's theory is:

$$t_1 = \frac{2\pi n^{*3}\hbar}{me^4 Z_o^2} ; \qquad t_2 = \frac{2\pi n^3 \hbar}{me^4 Z^2} . \qquad (31)$$

Approximately the total time for the complete orbit, t, is:

$$t = t_1 + t_2 = \frac{2\pi\hbar}{me^4} (n^{*3}/Z_o^2 + n^3/Z^2)$$

and the total average:

$$\overline{\left(\frac{1}{r^3}\right)} = \left\{ t_1 \cdot \overline{\left(\frac{1}{r^3}\right)}_1 + t_2 \cdot \overline{\left(\frac{1}{r^3}\right)}_2 \right\} : t . \qquad (32)$$

and using equations (30), (31)

$$\overline{\left(\frac{1}{r^3}\right)} = \frac{(Z + Z_o)Z^2 Z_o^2}{a_o^3\, l(l+1)(l+\tfrac{1}{2})(n^{*3}Z^2 + n^3 Z_o^2)} \qquad (33)$$

As $Z \gg Z_o$ in all but the lightest elements, equation (33) becomes:

$$\overline{\left(\frac{1}{r^3}\right)} = \frac{Z\, Z_o^2}{a_o^3\, n^{*3}\, l(l+1)(l+\tfrac{1}{2})} \qquad (34)$$

Then equation (34) together with equation (25) yield:

$$a_j = \frac{2\mu_I\mu_S ZZ_o^2}{a_o^3 n^{*3} (l + \tfrac{1}{2})j(j + 1)} \qquad (35)$$

According to Kopfermann[29] empirical values of Z are equal: to the atomic number for s-electrons, to the atomic number minus four for p-electrons, and about the atomic number minus eleven for d-electrons.

Again equation (35) may be shown to be valid for s-electrons, in which case it becomes:

$$a_s = \frac{16\mu_I\mu_S ZZ_o^2}{3a_o^3 n^{*3}}$$

When it is compared with equation (29) it suggests to write:

$$a_s = \frac{16\mu_I\mu_S\pi}{3} \psi_S^2(0) \qquad (36)$$

where:

$$\psi_S^2(0) = \frac{ZZ_o^2}{\pi a_o^3 n^{*3}} \qquad (37)$$

is a tentative way of expressing the s-electron density for r = 0 in a central field.

However, it is clear that this formula cannot be applied in the relativistic case since the s-electron density at the origin

tends to infinity, according to the Dirac's theory. Equation (37) therefore is expected to be valid for light elements and, in fact, it proves to be useful at least in the case of fine structure levels which can be represented by a Rydberg formula. Using relativistic quantum mechanics, Fermi and Segrè[15] found that in equation (36), $\psi_s^2(0)$ may be replaced by a $\psi_{eff}^2(0)$ calculated by means of the Darwin eigenfunctions. However, the actual computation of $\psi_{eff}^2(0)$ requires a knowledge of the eigenfunctions not only near the origin, and out of this region the uncertainties of numerical evaluation are specially noticeable. Therefore those authors discussed systematically the semi-empirical formula:

$$\psi_s^2(0) = \frac{Z}{\pi a_o^3 \rho^4} \cdot \frac{dE}{2Rh\, dn} \qquad (38)$$

where: R is the Rydberg constant,

$\rho = \sqrt{1 - \alpha^2 Z^2}$ with α standing for the fine-structure constant,

E is the energy of the terms expressed as a function of the quantum number n,

$1/\rho^4$ is a relativistic empirical correction.

When the relativistic correction is not taken into account

and when the fine-structure levels can be represented by a Rydberg formula, equation (38) reduces to the Goudsmit and Landé formula given by equation (37).

Equation (38) may also be written as:

$$\psi^2_0(0) = \frac{ZZ_o^2}{a_o^3 n^3 \rho^4}\left(1 - \frac{d\mu}{dn}\right) \qquad (39)$$

where $\left(1 - \frac{d\mu}{dn}\right)$ is known as the Fermi-Segrè factor, and

μ is the quantum defect.

To compute the Fermi-Segrè factor the method shown by Crawford and Schawlow[10] is generally followed. For terms fitting the Rydberg-Ritz formula (i.e. for unperturbed terms):

$$T = \frac{RZ_o^2}{(n - \mu)^2} \qquad (40)$$

with $\mu = \alpha + \beta T$

Then: $$\frac{d\mu}{dn} = \beta \frac{dT}{dn} = \frac{\beta}{\beta - \frac{n}{2T}} \qquad (41)$$

For electrons other than s, formula (35), generally called Goudsmit formula, has proved to be very useful. Some correction factors were introduced in it. Fermi and Segrè[15] have given a formula for $\overline{r^{-3}}$ in terms of the doublet separation $\Delta\nu$, in

general a very well known value from spectroscopic data. Their result is:

$$a_j = \frac{2\,l(l+1)\mu_I\,\Delta\nu}{Ij(j+1)(2\,l+1)\mu_s Z^*} \qquad (42)$$

where Z^* is defined by:

$$eZ^* = \overline{\left(\frac{1}{r}\frac{dV}{dr}\right)} \;:\; \overline{(r^{-3})}$$

Making a relativistic quantum mechanical treatment of the problem for the doublet S, P and D, Breit and Racah (see reference in Kopfermann[29]) found that equation (42) must be multiplied by the factor:

$$F_r(j,Z) = \frac{4j(j+\tfrac{1}{2})(j+1)}{\rho(4\rho^2-1)}$$

where $$\rho = \sqrt{(j+\tfrac{1}{2})^2 - \alpha^2 Z^2}$$

This relativistic factor is plotted in Atomic Spectra[30] as a function of Z and j.

Another correction factor which appears when computing $\overline{r^{-3}}$ using Dirac's theory, as pointed out by Kopfermann[29] and also

plotted in Atomic Spectra[30] as a function of Z and l, is $H_r(l,Z)$ and given by:

$$H_r(l,Z) = \frac{2\,l(l+1)}{2\,Z^2}\,(\rho' - \rho'' - 1) \qquad (44)$$

where: $$\rho' = \sqrt{(l+1)^2 - \alpha^2 Z^2}$$

and $$\rho'' = \sqrt{l^2 - \alpha^2 Z^2}$$

As seen from equations (43) and (44), $F_r(j,Z)$ and $H_r(l,Z)$ depend on $\alpha^2 Z^2$ and are appreciable only for large Z where the velocity of the electrons near the nucleus becomes comparable with the velocity of light, c.

Other correction factors arise from considering that the nucleus is not a point charge with a point magnetic moment. The first one, which is written as $(1 - \delta)$, was calculated by Crawford and Schawlow[10] chosing the nuclear model which best fitted the nuclear magnetic moment as measured by an induction method. They obtained:

$$\delta = \frac{2(j-\rho)\rho(2\rho+1)\,y^{2\rho-1}}{(2j-1)\Gamma^2(2\rho+1)} \qquad (45)$$

where $y = 2ZR/a_o$; R is the radius of the nucleus, and Γ is the gamma function.

This factor $(1 - \delta)$ must also multiply equation (42). Values of δ are plotted in Atomic Spectra[30] as a function of Z.

The second correction factor, $(1 - \varepsilon)$ takes account of the distribution of nuclear magnetic moment over the nuclear volume, and must multiply equation (42). This factor was computed in an approximate way by A. Bohr and Weisskopf (see reference in Atomic Spectra[30]) using an approximate relativistic electron density in the region of the nucleus for an s-electron. The result is:

$$\varepsilon \simeq \frac{ZR}{a} \left(\frac{a}{2ZR}\right)^{2(1-\rho)} \cdot \overline{(r^2/R^2)}$$

where the average must be taken over the distribution of magnetic moment; its value depends on the assumed nuclear model.

It is important to note that all correction factors are independent of the quantum number n. This result is due to the approximations made to compute them and means that these values would be correct only in the extreme case of very large quantum numbers. According to Kopfermann[29] significant deviations from the values given by the formulas written above do not occur if n is greater than six.

II - a - 3) Deviations from the interval rule

There are two major causes that produce departures from the interval rule: i) electric quadrupole terms, that is the electric

quadrupole energy interaction cannot be neglected in comparison with the magnetic dipole interaction energy; and ii) perturbations arising from neighbouring levels.

The starting point to find the eigenfunctions of an atom with several electrons given by Slater[43] is a model of an atom in which N electrons each move, without influencing each other, in the same central field with a potential energy - u(r). Only eigenfunctions that are antisymmetric in all pairs of electrons are used and therefore an eigenfunction is specified by giving a complet set of 5 N quantum numbers. These eigenfunctions are exact solutions of the quantum mechanical problem whose Hamiltonian is:

$$H_1 = \sum_{i}^{N} \left[\frac{1}{2\mu} \bar{p}_i^2 - u(r_i) \right]$$

while the Hamiltonian for the actual atom is:

$$H_2 = \sum_{i=1}^{N} \left[\frac{1}{2\mu} \bar{p}_i^2 - \frac{Ze^2}{r_i} + V(r_i)\bar{L}.\bar{S} \right] +$$

$$\frac{e^2}{2} \sum_{i \neq j} \frac{1}{r_{ij}}$$

This problem was treated by Condon[9].

Since H_1 and H_2 do not commute with each other the H_2 matrix will not be diago al when a representation based in the eigenfunctions of H_1 is used. Then to find the energy levels of an atom whose Hamiltonian is given by H_2 it is necessary to diagonalize its matrix. To calculate the eigenfunctions of H_2 in an approximate way it is possible to use perturbation theory considering that the perturbing operator is the difference between H_2 and H_1 :

$$V = \text{perturbing operator} = H_2 - H_1$$

The success of the calculation in the first order requires that the eigenvalues of H_2 yielded by a particular eigenvalue of H_1 remain close together compared with the distance of the particular eigenvalue of H_1 from its nearest neighbor in the spectrum of H_1.

If this condition is not fulfilled then the second order perturbation becomes important. An important second order correction implies that a non-negligible alteration of the eigenfunction has taken place so that, when it is expanded in terms of the eigenfunctions of H_1 it begins to have an important component of the eigenfunction of the neighboring level of H_1 in addition to the eigenfunction of the level from which it grew. Therefore as the second order correction becomes more important

the quantum numbers which were appropriate to label the different eigenvalues of H_1 become less and less appropriate for the labelling of the eigenvalues of H_2.

If ϕ_i are the eigenfunctions of H_1 and E_i its eigenvalues, in first order the eigenfunctions of H_2 are:

$$\psi_1 = \phi_1 + \sum_{i \neq 1} \frac{V_{1i}}{E_1 - E_i} \phi_i$$

where E_1 and E_i are the unperturbed energies and V_{1i} are the perturbation matrix elements between states 1 and i. These matrix elements will be zero if: i) the two states have different J, ii) the two states have different parity.

In hfs separations the interaction between different configurations is important since there are configurations even of high energy which are strongly coupled to the nucleus, in particular those which contain a relatively deep isolated electron in an s-state. If an eigenfunction ϕ_2 of this type is intermixed according to the first order perturbation theory, with another ϕ_1, having a small hfs, it may cause quite a large relative perturbation of the hfs constant, even if $V_{12}/(E_1 - E_2)$ is small. In some cases this perturbation may reverse the sign of the coupling constant of the state 1 even neglecting the effect of non-diagonal terms in the coupling with the nucleus,

which may in some cases be of the same or even larger order of magnitude.

II - b) Isotope shift

Isotope shift is considered in many books and papers. The general trend of ideas presented here are mainly taken from: Kopfermann[29], Stacey[44], White[54], Condon and Shortley[8], Kuhn[30] and Herzberg[19].

At present the isotope shifts are assumed to be mainly due to the finite nuclear mass and due to the distribution of nuclear electric density charge through the nuclear volume. In any of these two effects it is necessary to define a reference level in order to compare with it the shifts produced in the terms of an atomic system. This reference level is commonly chosen as the term energy appropriate to a point nucleus with infinite mass.

II - b - 1) Due to the finiteness of the nuclear mass

The additional energy that will be found in the reference term energy when the finite mass of the nucleus is considered, is given by its kinetic energy, as measured in the center of mass. It is assumed that the center of mass of the nucleus and electrons is at rest, which is the same as to say that the emitted photon carries away only a negligible amount of momentum. The momentum of the nucleus in the center of mass system is given by:

$$\bar{p}_N = -\sum_{i=1}^{n} \bar{p}_i \qquad (1)$$

where n stands for the whole number of electrons.

Whence:

$$E_m = \frac{\bar{p}_N^2}{2M} = \frac{1}{2M}\left(\sum_{i=1}^{n} \bar{p}_i\right)^2 \qquad (2)$$

where M is the finite mass of the nucleus.

$$E_m = \frac{1}{2M}\left(\sum_{i=1}^{n} \bar{p}_i\right)\cdot\left(\sum_{j=1}^{n} \bar{p}_j\right) = \frac{1}{2M}\sum_{i,j=1}^{n} \bar{p}_i\cdot\bar{p}_j =$$

$$= \frac{1}{2M}\sum_{i=1}^{n} \bar{p}_i^2 + \frac{1}{2M}\sum_{i>j}^{n} \bar{p}_i\cdot\bar{p}_j \cdot \qquad (3)$$

The first term in equation (3) gives the Bohr reduced mass correction and the additional energy is called "the normal mass shift".

Quantum mechanically E_m should be considered as an operator. When solving the Schrodinger equation it will appear:

$$\left(\frac{1}{2M}\sum_{i=1}^{n} \bar{p}_i^2 + \frac{1}{2m}\sum_{i=1}^{n} \bar{p}_i^2 + \sum_{i>j}^{n} \bar{p}_i\cdot\bar{p}_j + V\right)\emptyset = E\emptyset \qquad (4)$$

where m is the mass of an electron.

Omitting the cross terms, equation (4) becomes

$$\left[\tfrac{1}{2} \left(\frac{M + m}{Mm} \right) \sum_{i=1}^{n} \vec{p}_i^{\,2} + V \right] \phi = E \phi$$

or

$$\left[\frac{1}{2\mu} \sum_{i=1}^{n} \vec{p}_i^{\,2} + V \right] \phi = E \phi \qquad (5)$$

where μ is the reduced mass.

Then the eigenvalues of the energy are equal to those obtained when an infinite nuclear mass is considered, multiplied by $M/(M + m)$. The only cases in which the cross terms do not appear are in hydrogenic atoms. In such cases the term values are given by:

$$T = \frac{R_\infty Z^2}{mn^2} \mu = \frac{R_\infty Z^2}{n^2} \cdot \frac{M}{M + m} = T_\infty \cdot \frac{M}{M + m} = T_\infty \cdot \frac{1}{1 + m/M}$$

$$\simeq T_\infty \left(1 - \frac{m}{M}\right) = T_\infty + \Delta_N T \qquad (6)$$

If there are two isotopes whose nuclear masses are M and M' the difference between the corresponding terms is:

$$\delta (\Delta_N T) = T_\infty \left(1 - \frac{m}{M}\right) - T_\infty \left(\frac{m}{M'} - \frac{m}{M}\right).$$

If mass defects are neglected:

$$\delta(\Delta_N T) = T_\infty (m/p)\left(\frac{1}{A'} - \frac{1}{A}\right) = T_\infty (m/p)\left(\frac{A - A'}{AA'}\right) = T_\infty m \cdot \frac{\Delta A}{A^2 p} \quad (7)$$

where p is the proton mass and A is the mass number.

Then the difference between corresponding term values for two different isotopes decreases as A^{-2}, and therefore is much smaller for heavy atoms than for light ones.

From equation (6) it is apparent that the normal mass shift reduces the term value (increases the energy of the level) and this effect is the smaller the heavier the atom. Thus, the line due to the heavier isotope has a greater wave-number (see fig. II - 2) than the line due to the lighter one.

The cross terms in equation (3) depend on the relative movement of the electrons inside the atom. The shift produced by these terms is called "the coupling effect" or "the specific mass shift". While the normal mass effect always yields a reduction in the term values, the coupling effect may produce a shift opposite or in the same direction as the normal mass effect.

The specific mass effect is very difficult to evaluate. Only in the lighter atoms a good agreement between theory and experiment was achieved.

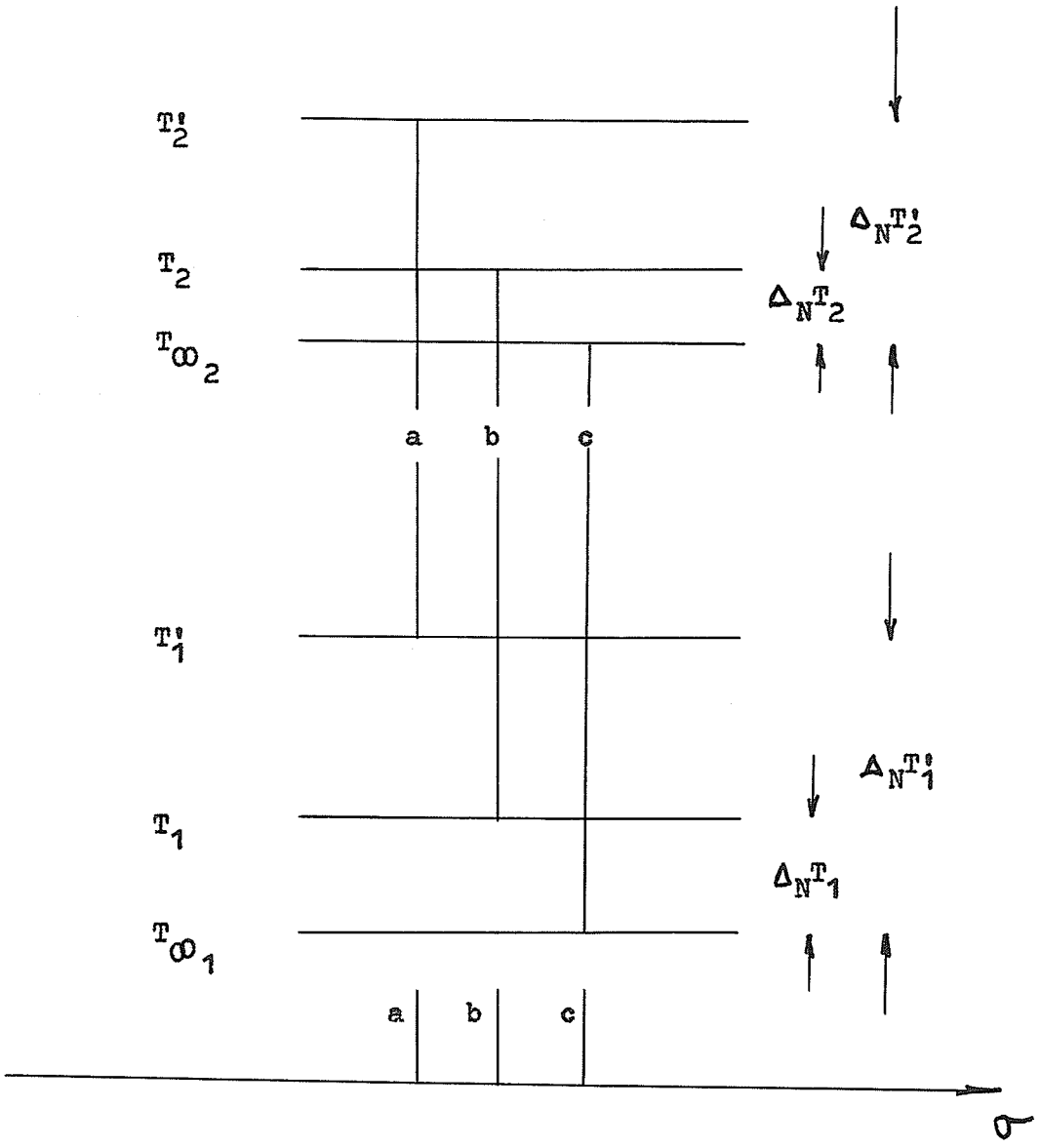

Fig. II - 2) Normal mass shift. T_{∞_1} and T_{∞_2} are two terms in an atom whose nuclear mass is assumed to be infinity. If this specimen has two isotopes, the corresponding terms are marked T_1 and T_2 for the lighter one, T'_1 and T'_2 for the heavier one. The normal mass shifts are given by eq. (6). a, b and c are the corresponding transitions in a wavenumber scale. a belongs to the lighter isotope, b to the heavier one, and c to the atom with nuclear mass equal to infinity.

The theoretical calculation is determined using the cross terms $\frac{1}{2M} \sum_{i>j} \bar{p}_i \cdot \bar{p}_j$ as a perturbation. The unperturbed energy is that obtained by taking the normal mass shift into account.

As $\bar{p}_i = -i\hbar \bar{\nabla}_i$, $\bar{p}_j = -i\hbar \bar{\nabla}_j$ the first order perturbation theory gives:

$$\Delta_s T = -\frac{\hbar^2}{M} \sum_{i>j} \int \psi^* \bar{\nabla}_i \cdot \bar{\nabla}_j \psi \, d^3r \qquad (8)$$

where ψ are the eigenfunctions of the unperturbed system.

To compute $\Delta_s T$ some assumption must be made for the wave functions of the non-perturbed system. For example, in Ne calculations were carried out using a Hartree field (see references in Condon and Shortley[8] p.419) and only a qualitative agreement with the observations was obtained. In heavier elements the agreement comes poorer (see references in Kopfermann[29], p. 165). Using the Slater's approximation[43] equation (8) may be written as a sum of integrals using instead of ψ, pairs of single electron central field functions. These integrals are called "specific mass integrals".

By means of equation (8), in analogy with equation (6), the term value may be written:

$$T = T_\infty + \Delta_N T + \Delta_s T \qquad (9)$$

The normal mass shift produced in the components of a line in three consecutive isotopes of the same element are in the same ratio as the masses of the nucleus of the first and third isotope. According to equation (7):

$$\Delta_N T = T_\infty \frac{m}{p} \left(\frac{A_1 - A_2}{A_1 A_2} \right)$$

hence:

$$\Delta\sigma_{12} = \frac{m}{p} \left(\frac{A_1 - A_2}{A_1 A_2} \right) \sigma$$

where $\Delta\sigma_{12}$ is the difference in wave-number between the corresponding transitions in the isotopes of mass numbers A_1 and A_2 and is the wave-number of the line under consideration, assuming the nucleus has an infinite mass.

Similarly:

$$\Delta\sigma_{23} = \frac{m}{p} \left(\frac{A_2 - A_3}{A_2 A_3} \right)$$

But $A_2 - A_3 = A_1 - A_2 = 1$ since they are consecutive isotopes.

Whence:

$$\frac{\Delta\sigma_{12}}{\Delta\sigma_{23}} = \frac{A_3}{A_1} \qquad (10)$$

According to the calculations performed by Hughes and Eckart[21] the same relation appears for the helium like atoms, taking into account the specific mass shift.

The table in p. 166 of Nuclear Moments[29] shows the mass effects measured by several authors and indicates that when A is near 85 the normal and the specific mass effects become of the same order as the experimental errors in interference spectroscopy.

II - b - 2) Due to the distribution of the nuclear electric charge

This effect is commonly refered to as "the nuclear volume effect" or "the field effect" and it arises because the nuclear charge is distributed through a finite volume. To a first approximation the nucleus may be imagined as a sphere whose radius R depends on the mass number A according to:

$$R = R_o \cdot A^{1/3} \qquad (1)$$

the value of the constant R_o now is accepted to be 1.2×10^{-13} cm as given by measurements of the scattering of fast electrons by nuclei. The finite nuclear radius makes the potential in which the atomic electrons move differ from that produced by a point nucleus. This modification of the potential depends on R_o and A. Therefore, different isotopes with different mass numbers have different energy levels. For distances r from the center of the nucleus larger than R, the potential is a Coulomb potential, given by - Ze/r (in e.m.u.) where Z is the atomic

number and e is the absolute value of the electronic charge. For r smaller than R the form of the potential depends on the chosen nuclear model. The charge enclosed in a sphere of radius r is given by:

$$q(r) = \int_0^r \rho(x) . 4\pi x^2 dx \qquad (2)$$

where $\rho(x)$ is the charge density as a function of x, the distance to the center of the nucleus. The nuclear potential is:

$$V(r) = - \frac{Ze}{R} - \int_r^R q(r') \, dr'/r'^2 \qquad (3)$$

where q(r') is given by equation (2), and r is smaller than R. If r is greater than R then the potential seen by the electron is $V_o(r) = - Ze/r$ (4)

To compute the shift produced in an energy term by the departure of the Coulomb potential inside the nucleus, first order perturbation theory may be used. The unperturbed system is considered to be the atom with a point nucleus, i.e. it is assumed that the electron is moving in an electrostatic potential given by equation (4), for any value of r. The perturbing operator is given by the difference between equations (3) and (4), and the shift produced in the energy term is:

$$\Delta E_{is} = \int_0^R \phi^*(r) \left[V(r) - V_o(r) \right] \phi(r) \, 4\pi r^2 dr \qquad (5)$$

where $\phi(r)$ are the unperturbed eigenfunctions computed with a point nucleus.

Bartlett[2], following this line of reasoning, considered the isotope shift in Tl^{203} and Tl^{205}, where he considered that the Tl nucleus with $I = \frac{1}{2}$, could have neither a permanent electric dipole or a permanent higher electric moment, and therefore, the hfs displacement should be due to a difference in the radial dependence of the potential. To solve equation (5) he adopted the model: $V(r)$ = constant if $r < R$ and $V(r) = -Ze/r$ if $r > R$. He assumed that the potential V = constant is the same for both isotopes. For the eigenfunctions $\phi(r)$ in equation (5) he used hydrogenic ones without taking into account any screening of the nucleus by the electron core or any relativistic correction and suggested that in order to get a better agreement with the experimental results, $V(r)$ = constant for $r < R$ could be varied to fit the calculations with the experimental data. He concluded that there is no difficulty in accounting for the isotope shift using the hypothesis that the deviations from the Coulomb's law in the neighborhood of the nucleus are responsible for such effect.

Almost simultaneously Racah[40] and Rosenthal and Breit[41] used relativistic eigenfunctions to solve equation (5). Rosenthal and Breit made calculations in the S-terms of Hg and their results are in agreement with those of Racah. They also

calculated the effect of the deviations of the nuclear field from the Coulomb's law on the interaction of the electron with the nuclear spin. They started by solving the central field equations for the Darwin-Gordon radial functions ϕ_1 and ϕ_2 for Dirac's equation considering a potential V(r) = constant if $r < R$ and a potential following the Coulomb's law outside the nucleus, i.e. if $r > R$. In both cases they made the approximation $E/mc^2 = 1$, i.e. the term value energy is negligible in comparison with mc^2, the rest energy of the electron. In equation (5) as eigenfunctions they used the limit case for ϕ_1 and ϕ_2 when R = 0, functions which are called ϕ_1^o and ϕ_2^o and were normalized to:

$$\int_0^{\infty} (\phi_1^{o\,2} + \phi_2^{o\,2})dr = 1$$

In this way they obtained:

$$E_{is} = \frac{2e^2ZC^2j(j-\rho)}{\hbar^2(2\rho+1)} \left[y_o^{2\rho} + (v/2a)y_o^{2\rho+1} \right] \frac{\Delta y_o}{y_o}, \quad (6)$$

where:

C is a constant to be determined,

Z is the atomic number,

$a = \alpha Z$ with α = fine structure constant,

v is the potential energy in mc^2 units,

j is the quantum number,

$$y_o = 2\frac{mZe^2R}{\hbar^2} \quad \therefore \quad \Delta y_o = 2\frac{mZe^2}{\hbar^2}\Delta R$$

$$\frac{\Delta y_o}{y_o} = \frac{\Delta R}{R}$$

ΔR is the change in the nuclear radius from one isotope to the next one,

$\rho = \sqrt{1 - Z^2\alpha^2}$ and Γ is the gamma function.

For S-terms the constant C was expressed in terms of the value $\psi^2(0)$ which is the square of the non-relativistic Schrödinger function at r = 0. In this case equation (6) becomes:

$$\Delta E_{is} = \frac{4\pi R_\infty a_o^3 \psi^2(0)\,(1+\rho)}{Z\Gamma^2(2\rho+1)} \left[y_o^2\rho + (v/2a^2)y_o^2\rho + 1 \right] \frac{\Delta y_o}{y_o}, \quad (7)$$

this equation may be written (see Crawford and Schawlow[10]):

$$\Delta E_{is} = \frac{4\pi R_\infty a_o^3 \psi^2(0)}{Z} \cdot \frac{1+\rho}{\Gamma^2(2\rho+1)} \cdot y_o^{2\rho} \frac{\Delta y_o}{y_o} \cdot B \quad (8)$$

where the B factor depends on the potential inside the nucleus. In the case of equation (7) this factor takes the expression:

$$B = 1 + vy_o/2a^2 \quad (9)$$

If the potential v (i.e.: $V(r)/mc^2$ for $r < R$) is a constant for a given nucleus, but a function of y_o, the B factor takes the expression:

$$B = 1 + \frac{vy_o}{2a^2} + \frac{y_o^2}{2a^2(2\rho + 1)} \cdot \frac{dv}{dy_o} \qquad (10)$$

If the whole nuclear charge is considered to be distributed only on the surface of the nucleus, the B factor takes the simple form : (this model is sometimes called "the top slice model"):

$$B = \frac{1}{2\rho + 1} \qquad (11)$$

If the addition of neutrons does not change the proton distribution, then instead of equation (11) the factor B is zero.

Other common model for the distribution of the electrical charge inside the nucleus is to assume that the nuclear charge is uniformly distributed throughout the nuclear volume. In this case, one has:

$$B = \frac{3}{(2\rho + 1)(2\rho + 3)}$$

and equation (3) becomes:

$$V(r) = \left[-3/2 + \tfrac{1}{2} \left(\frac{y}{y_o}\right)^2 \right] \frac{2a^2}{y_o}. \qquad (13)$$

These B values were obtained by solving the wave equation in the region $r < R$ for the particular potential shapes. Earlier than Crawford and Schawlow[10], in 1945, (see reference in Breit[5])

Broch gave a correction factor to be applied to the perturbation theory result, based on one model. In any event, the electron wave functions evaluated by the authors of both papers (Broch and Crawford and Schawlow[10]) depend on the assumed nuclear charge distribution and are difficult to obtain except for the simplest nuclear models.

Equation (8) may be split in two factors: one depending only on the electronic wave functions and the other one depending only on the nuclear properties (see, for instance, Stacey[44], Hindsmarsh[20], Kopfermann[29] or Kuhn[30]):

$$\Delta E_{is} = \frac{\psi^2(0)\pi a_o^3}{Z} \cdot \frac{4R_\infty(1+\rho)}{(2\rho+1)} \cdot (2ZR/a_o)^2 \cdot \frac{\Delta R}{R} \cdot B =$$

$$= \frac{\pi a_o^2}{Z} \psi^2(0) \cdot C(Z,R,\Delta R/R). \qquad (14)$$

Regarding the nucleus as an uniformly charged sphere, B is given by equation (12) and the C factor in equation (14) becomes:

$$C(Z,R,\Delta R/R) = \frac{12\, R_\infty(\rho+1)}{(2\rho+1)(2\rho+3)\Gamma^2(2\rho+1)} \cdot \left(\frac{2ZR}{a_o}\right)^{2\rho} \cdot \frac{\Delta R}{R} \cdot \qquad (15)$$

Similarly, for a spherical nucleus with surface charge, it is found (using equation (11)):

$$C(Z,R,\Delta R/R) = \frac{4R_\infty(\rho+1)}{(2\rho+1)\Gamma^2(2\rho+1)} \left(\frac{2ZR}{a_o}\right)^{2\rho} \cdot \frac{\Delta R}{R} \qquad (16)$$

which is $(2\rho + 3)/3$ times larger than equation (15).

According to the liquid drop model, the mass number A, and the radius R of a nucleus are connected through equation (1). Then:

$$\frac{\Delta R}{R} = \frac{\Delta A}{3A}$$

From one isotope to the next one, $\Delta A = 1$. Then equation (16) is a very slowly decreasing function of A, varying as: $A^{2\rho/3 - 1}$; being near 1 for most nuclei. According to Kuhn[30] for Z = 50, $\rho = 0.93$ and when Z = 90, $\rho = 0.75$.

In order to compute equation (14) it is necessary to know $\psi^2(0)$. The quantity $C(Z,R,\Delta R/R)$ depends only on nuclear properties, then for two isotopes of the same element is should be independent of the electron configuration and of the degree of ionization of the atom, i.e.

$$C(Z,R,\Delta R/R) = \frac{\Delta E_{is}}{(a_o^3/Z)\pi\psi^2(0)} \qquad (17)$$

is a characteristic constant for the isotope pair and does not depend on the multiplet term considered.

To evaluate $\psi^2(0)$ in equation (17), in spite of its drawbacks, the Fermi-Segrè formula (see section a in this chapter) seems to be still the method most commonly used. This method

does not take into account the configuration interaction, nor the exchange effects, nor the screening effects by electrons outside closed shells. A thorough discussion of its limitations and corrections was undertaken by Breit[4]. In this work there detailed references to papers showing experimental support of the Fermi-Segrè formula, though, it is indicated there that tests of the applicability of the formula based on the measured hfs cannot be trusted since configuration interaction does not affect isotope shifts in the same way as hfs splittings. Therefore the experimental determination of $\psi^2(0)$ measuring magnetic hfs splittings is restricted only to the class of lines of an odd isotope with known g(I) which its hfs has been measured, and both effects, the magnetic hfs and the isotope shift, are due to an unpaired s-electron. This does not happen, for example, in the case when a configuration nsmd is perturbed by the configuration ns^2, since the perturbation contributes to the isotope shift but not to the magnetic hfs, and, therefore the calculated $\psi^2(0)$ would yield a wrong result.

It is common to define from equation (17) an experimental value of $C(Z,R,\Delta R/R) = C_{exp.}$ but only in very few lines it is possible to get the $C_{exp.}$ with rather good accuracy and very often no values of this parameter can be given.

In Kopfermann[29] it is shown for different ns terms in the

alkali-like spectrum of Tl III how far the proportionality between ΔE_{is} and the electron charge density at the nucleus is satisfied.

Similarly to the $C_{exp.}$ defined above, using equation (14) and some specific nuclear model, a $C_{th.}$ is defined. In the case of a uniformly charged sphere, $C_{th.}$ is given by equation (15). In the top slice model, $C_{th.}$ is given by equation (16). In the literature it is common to find $C_{exp.}/C_{th.}$ plotted against N, the neutron number, aiming to test the theory used. Generally it appears that the magnitudes predicted by the theory remain somewhat greater than the isotope shifts revealed by experimental results, and that the points do not lie on a horizontal line but form a curve with a sharp peak at N = 90 and minima near 80 and 120. The large fluctuations are exhibitted even within the isotopes of one element. Experimentally it is also known that the spectral lines of an isotope of odd mass number do not lie midway between the lines of the neighbouring isotopes of even mass number, but are shifted towards the even isotope of lower mass number, a fact known as odd-even staggering. The even isotopes are not equally spaced either and when the sharp peak appears near N = 90, these shifts are markedly large.

First order perturbation theory is not a good approximation for the calculation of isotope shifts, since the fields responsible for the perturbation energy are very large, even though they act in a small region. Rosenthal and Breit[41] discussed

this problem after applying that method using a constant potential inside the nucleus and taking the same for both isotopes.

Treatments given by Broch in 1945 and Bodmer in 1953 (see references given by Hindsmarsh[20]) avoid the use of the perturbation method and permit the derivation of an expression for the isotope shift which is not dependent on the assumption that the perturbed wave functions differ only slightly from the unperturbed ones in the region of the perturbation. Using Broch's method Crawford and Schawlow[10] calculated the isotope shift for an s-electron in Tl, using the top slice model and the uniformly charged nucleus. Comparing their results with those obtained using perturbation theory they found an error of 36 % and 34 %, respectively for both models.

The irregularities observed in the plot $C_{exp.}/C_{th.}$ vs N, especially near the neutron numbers N = 90 and N = 126 are considered to be due essentially to the departure of the nuclear charge distribution from spherical symmetry, and to the fact that this nuclear deformation can change from one isotope to another. Usually it is assumed that the deformation is produced while the charge density of the nucleus is kept constant. The equation for its ellipsoidal shape is given by:

$$r(\Theta) = R\left[1 + \beta\,(3/2\,\cos^2\Theta - 1/2)\right] N\beta$$

where Θ is the angle between the radius and the symmetry axis,

R is the radius of the undeformed spherical nucleus of equal volume,

β is a parameter characterizing the deformation. For a prolate ellipsoide, with its major axis along the symmetry axis, $\beta > 0$ and the semi-axis of the ellipsoid are given by: $a = R(1 + \beta)$ and $b = R(1 - \frac{1}{2}\beta)$.

N_β is a normalization constant chosen to fit the requirement of incompressibility of nuclear matter.

When the deformation effect is compared with that of a uniform spherical charge distribution, E_{is} is found to be proportional to

$$\Delta N \times \frac{\partial(\beta^2)}{\partial N} \qquad (18)$$

if the leading terms only in the nuclear radius are considered. This result applies only to s-electrons.

Deformation of nuclei with neutron number between the magic numbers, 82 and 126, are known from Coulomb excitation and level structure (Kuhn[30]) so the derivative appearing in equation (18) may be calculated.

The quadrupole moment connected with β^2 is that corresponding to the intrinsic neclear deformation rather than to the measured quadrupole moment (see Kopfermann[29] p. 187). If the intrinsic quadrupole moment is Q_o and Q is the measured quadrupole moment, they are connected by:

$$Q = \left[\frac{(I + 1)(2I + 3)}{I\,(2I - 1)}\right]^{-1} Q_o \qquad (19)$$

If I = 0 the average component of a vector along the axis of symmetry is zero in any direction because the projection on the spin axis vanishes. Therefore in this case the quadrupole moment cannot be observed directly. If I = ½ the nucleus may also have an intrinsic quadrupole moment, but it becomes spread out by the precession about the axis of symmetry into a charge distribution of spherical symmetry, showing a Q = 0. This is the case in Cd^{111} and Cd^{113}.

When neutrons form a closed shell the parameter ρ is equal to zero. Then considering that deforming effects are only due to neutrons at the magic numbers N = 82 and N = 126 the nucleus should be expected to be spherically symmetric and the quadrupole contribution to ΔE_{is} may be expected to be large when N is near one of those numbers. When a shell is almost closed the quadrupole moment is negative and just after the shell is closed the quadrupole moment is positive. In the latter case the ΔE_{is} should be large since the quadrupole effect is in the same direction as the effect of general expansion of the nuclear volume. On the other hand, in the former case the ΔE_{is} should be small since the quadrupole effect has opposite sign to that of the general expansion of the nuclear volume.

A further improvement may be found by taking into consideration the screening of the inner electrons by the valence electron.

Since an s-type valence electron has a finite probability of being near the nucleus, the probability of finding it inside the orbit of any of the inner electrons is not negligible. During the period in which the valence electron remains inside the orbit of an inner electron, the effective nuclear charge for the inner electron is reduced by one unit. This reduction in the binding force between the nucleus and the inner electron means that the contribution of the inner electron to the isotope shift of the entire atom is diminished. A small fractional change in the inner electron isotope shift yields an appreciable fraction of the isotope shift of the valence electron, since the former is closely bound to the nucleus.

Crawford and Schawlow[10] have estimated this screening effect. A direct calculation of this effect requires an accuracy in $\psi^2(0)$ of the inner electrons which is not possible with the Hartree self-consistent field functions. They have calculated, for Hg, the probability that the 6s valence electron is closer to the nucleus than the inner s-electrons, and found that the observed shift is 16 % smaller than that calculated neglecting the screening effect. Not only are the inner s-electrons screened by the 6s electron, but, p and d inner electrons are also affected. However, they estimated that p and d electrons have very small isotope shifts and therefore the screening of them by the valence electron has a negligible effect on the shifts.

Chapter III

THE BREADTH AND SHAPE OF SPECTRAL LINES

The breadth and shape of spectral lines are mainly due to the following factors: (a) the natural width, (b) the Doppler broadening, and (c) broadening caused by interactions between the radiating atom and its neighbors.

III - a) The natural or radiation breadth

In most simple cases the radiation breadth may be calculated by using a classical picture. In resonance lines, specially in alkali atoms, the classical results and those obtained with a quantum mechanical calculation are found to agree within the limits of errors.

The classical approach based on the Lorentz's theory of electrons, is given in several books and papers. The sketch given here follows the ideas developed by Stone[45], White[54], Kuhn[30] and Lorentz[33].

An atom with an electron and the nucleus at rest is considered. In the classical picture the electron obeys Newton's second law. The forces acting upon the electron are the elastic binding force and the radiation force. To see if the last one may be neglected, the criterion given by Jackson[22], chapter 17,

is adopted here.

To find an expression for the radiative force[33] an electron moving along the x-axis with non constant velocity is considered. It is necessary to compute the field produced at a point $P(x',y',z')$ inside the electron due to its own charge. To find this field, the scalar and vector potential must be calculated (see fig. III - 1)

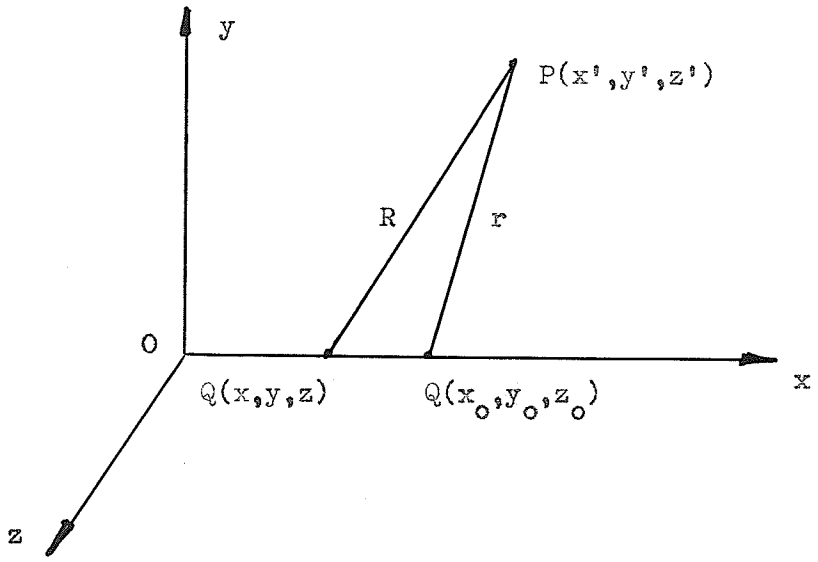

Fig. III - 1) $Q(x,y,z)$ is the retarded position of the charge $d\varrho$ which produces the field $\bar{E}$ in $P(x',y',z')$ at time t. $Q(x_o,y_o,z_o)$ is the present position of $d\varrho$, i.e. it is the position of $d\varrho$ at time t. $P(x',y',z')$ is the observation point inside the volume of the electron.

The time taken by $d\rho$ for going from $Q(x,y,z)$ to $Q(x_o,y_o,z_o)$ is

$$\tau = \frac{R}{c} = \frac{1}{c}\left[(x' - x)^2 + (y' - y)^2 + (z' - z)^2 \right]^{1/2}. \quad (1)$$

If v, $\dot{v}$, $\ddot{v}$, etc. are assumed to be small enough to neglect second order effects, τ has the approximate value:

$$\tau \simeq \frac{r}{c} \qquad (1)'$$

The retarded position may be expanded in a series in terms of the present conditions:

$$x = x_o - v_o\tau + \tfrac{1}{2}\dot{v}_o\tau^2 - \frac{1}{6}\ddot{v}_o\tau^3 + \frac{1}{24}\dddot{v}_o\tau^4 \ldots \quad (2)$$

and according to (1)':

$$x = x_o - v_o\frac{r}{c} + \dot{v}_o\frac{r^2}{2c^2} - \ddot{v}_o\frac{r^3}{6c^3} + \dddot{v}_o\frac{r^4}{24c^4} - \ldots \quad (3)$$

Similarly the retarded velocity in terms of the present one is

$$v = v_o - \dot{v}_o\frac{r}{c} + \ddot{v}_o\frac{r^2}{2c^2} - \ldots \quad (4)$$

which was written taking the time derivative of (2) and replacing τ by $\frac{r}{c}$.

The potential in $P(x',y',z')$ are given by :

$$\phi(x',y',z') = \left[\int \frac{\rho}{r}\, d^3r\right]_{ret.} \quad ; \quad \bar{A}(x',y',z') = \frac{1}{c}\left[\int \frac{\bar{v}}{r}\rho\, d^3r\right]_{ret.} \quad (5)$$

where ret. means that these expressions must be evaluated at time $t - \tau$. The integral must be carried over the whole space occupied by the electron.

Carrying equation (2) into (1) and keeping only first order terms in v_o, $\dot{v}_o$, etc. it is found:

$$\tau = \frac{r}{c} - \frac{v_o}{c^2}(x_o - x') + \frac{\dot{v}_o}{ac^3}(x_o - x')r - \frac{\ddot{v}_o}{6c^4}(x_o - x')r^2 - \ldots \qquad (6)$$

The volume element is:

$$d^3r)_{ret.} = dx.dy.dz,$$

from equation (3)

$$dx = \left\{1 - \frac{v_o}{c} \cdot \frac{x_o - x}{r} + \frac{\dot{v}_o}{c^2}(x_o - x') - \frac{\ddot{v}_o}{2c^3}(x_o - x')r + \ldots \right\} dx_o \qquad (7)$$

whence:

$$d^3r)_{ret.} = \{\}\, d^3r_o \quad \text{and} \quad \frac{d^3r}{r})_{ret.} = \{\}\frac{d^3r_o}{c\tau_o} \qquad (8)$$

replacing τ by its value given in equation (6) and keeping only first order terms in v_o, $\dot{v}_o$, etc. the retarded volume element is given by:

$$\frac{d^3r}{r})_{ret.} = \frac{d^3r}{r}\left\{1 + \frac{\dot{v}_o}{2c^2}(x_o - x') + \frac{\ddot{v}_o}{3c^3}(x_o - x')r + \ldots\right\} \qquad (9)$$

putting this expression into equation (5) and calculating the x-

component of the electric field:

$$E_x = -\nabla_x \phi - \frac{1}{c}\frac{\partial A_x}{\partial t} = \int \rho \frac{(x_o - x')}{r^3} \, d^3r + \frac{\dot{v}_o}{2c^3} \int \left[\frac{1}{r} + \frac{(x_o - x')^2}{r^2}\right] \rho \, d^3r$$

$$- \frac{2\ddot{v}_o}{3c^3} \int \rho \, d^3r \qquad (10)$$

To find the force the following integral must be performed:

$$F_x = \int \rho E_x \, d^3r \qquad (11)$$

Substituting equation (10) into equation (11), it is found that the first term cancels out; the second one gives a quantity proportional to the acceleration of the electron and depends upon the charge distribution inside the electron; and the last one gives a term of the form:

$$\frac{2e^2\ddot{v}_o}{3c^3} \qquad (12)$$

which is the reaction force and is independent of the charge distribution inside the electron.

It is worthwhile to note that equation (12) can be found imposing the following conditions upon the radiation force: i) It is zero if no acceleration is present, since in such case there is no radiation, ii) It is proportional to e^2, where e is

the electron's charge, since the radiated power is proportional to e^2, and, the radiation force cannot depend on the sign of the charge, iii) In the radiation force a factor $t_o = (2e^2)/3mc^3$ appears. This factor is the characteristic time defined in Jackson[22] to adopt a criterion about the impossibility of neglecting the radiation force, iv) The work done by the radiation force is equal in modulus to the energy radiated in the same interval of time.

The equation of motion of the radiating electron bound to the nucleus is given by:

$$\frac{d^2\bar{r}}{dt^2} + \frac{k}{m}\frac{d\bar{r}}{dt} - \frac{2e^2}{3c^3}\cdot\frac{d^3\bar{r}}{dt^3} = 0 \qquad (13)$$

where $\bar{r}$ is the position vector from the stationary nucleus to the instantaneous position of the electron, and k is a constant of proportionality between $\bar{r}$ and the elastic binding force.

To solve equation (13) the radiation force is assumed to be small compared with the other two terms, though not small enough to be neglected. Then, as an approximation one has:

$$\bar{r} = \bar{A}\, e^{iw_o t}\, e^{-\frac{1}{2}w_o^2 t\tau} + \bar{B}\, e^{-iw_o t}\, e^{-\frac{1}{2}w_o^2 t\tau} \qquad (14)$$

where:

$w_o = \frac{k}{m}$, $\tau = (2e^2)/3mc^3$, and $\bar{A}$ and $\bar{B}$ are vectorial constants.

Equation (14) represents an elliptical spiral converging towards the equilibrium position. The exponential damping reduces the amplitude of the motion to e^{-1} when $t = 2/w_o^2 \tau = 2/\gamma$ (15). To estimate γ in visible light it must be remembered that $\tau \cong 6 \times 10^{-24}$ sec. If $\lambda = 5000$ Å then:

$$\gamma_{5000\ \text{Å}} \cong 10^{-8} \text{ sec.} \qquad (16)$$

The spectrum of the emitted radiation is given by (see section 14.5 of Jackson[22]):

$$\frac{dI(w)}{d\Omega} = \frac{e^2 w^2}{4\pi^2 c^3} \left| \int \bar{n} \times (\bar{n} \times \dot{\bar{v}})\, e^{iw(t - \bar{n}\cdot\bar{r}(t)/c)}\, dt \right|^2 \qquad (17)$$

where: $\frac{dI(w)}{d\Omega}$ is the energy radiated per unit of solid angle per unit frequency interval.

$\bar{n}$ is a vector with modulus equal to 1, directed along the line connecting the retarded position of the particle and the observation point.

$\bar{r}(t)$, as before, is the position vector of the electron.

A cartesian co-ordinates system with the nucleus at origin, P (observation point) on the z-axis and the motion of the electron in the (x,y) plane is chosen. Then using equation (14) one obtains:

$$\bar{v} \cong i\bar{A}w_o\, e^{(iw_o - \frac{1}{2}w_o^2\tau)t} + i\bar{B}w_o\, e^{(-iw_o - \frac{1}{2}w_o^2\tau)t} \qquad (18)$$

$$\dot{\bar{v}} \cong -\bar{A}\, w_o^2\, e^{(iw_o - \frac{1}{2}w_o^2\tau)t} - \bar{B}\, w_o^2\, e^{(-iw_o - \frac{1}{2}w_o^2\tau)t}$$

where the approximation is taken using $w_o^2\tau \ll w_o$.

With P far from the origin, $\bar{n}$ is approximately constant and directed along the z-axis. Then, substituting equation (18) into equation (17), and performing the calculations the following result is obtained:

$$\frac{dI(w)}{d\Omega} = \frac{e^2 w_o^4}{4\pi^2 c^3}\left\{\left|\frac{A_x}{\frac{1}{2}w_o^2\tau - i(w_o + w)} + \frac{B_x}{\frac{1}{2}w_o^2\tau - i(w - w_o)}\right|^2 + \right.$$

$$\left. + \left|\frac{A_y}{\frac{1}{2}w_o^2\tau - i(w + w_o)} + \frac{B_y}{\frac{1}{2}w_o^2\tau - i(w - w_o)}\right|^2\right\}. \qquad (19)$$

In equation (19) the first and third terms in the curled brackets give a narrow peak at $w = -w_o$, while the second and fourth terms give a narrow peak at $w = w_o$. These peaks are narrow since $\frac{1}{2}w_o^2\tau \ll w_o$. As the frequency w is always positive only the second and fourth terms will be considered. They yield:

$$\frac{dI(w)}{d\Omega} = \frac{e^2 w_o^4}{4\pi^2 c^3} \cdot \frac{B_x^2 + B_y^2}{\frac{1}{4}\gamma^2 + (w - w_o)^2} = \frac{dI(w_o)}{d\Omega} \cdot \frac{\frac{1}{4}\gamma^2}{\frac{1}{4}\gamma^2 + (w - w_o)^2} \qquad (20)$$

This spectrum of frequencies is called a Lorentz profile.

When many atoms are present a statistical average yields an equation of the same form as equation (20).

The half width of this curve (defined as the interval between the two points where the intensity drops to half its maximun value) is found from equation (20):

$$\frac{1}{2} = \frac{\gamma^2}{4\left[(w - w_o)^2 + \frac{1}{4}\gamma^2\right]}$$

hence:

$$w_{1,2} = w_o \pm \frac{1}{2}\gamma$$

and the half width is:

$$\delta_w = w_1 - w_2 = \frac{2e^2 w_o^2}{3mc^3} \qquad (21)$$

In equation (21) it is apparent that the half-intensity breath is proportional to the square of the frequency, i.e. in a frequency or wave-number scale the "natural width" is wider the higher the frequency. On the other hand, when using a wave-length scale, since

$$\frac{w_1 - w_2}{w_o} = \frac{\lambda_1 - \lambda_2}{\lambda_o}$$

the half width is:

$$\delta_\lambda = \lambda_1 - \lambda_2 = \lambda_o\left(\frac{W_1 - W_2}{W_o}\right) = \frac{4\pi e^2}{mc^2} \qquad (22)$$

which is independent of the frequency and whose value is about 10^{-4} Å for any wavelength.

Equation (21) gives the half width in a 2π times frequency scale. To change to a wave-number scale it is:

$$\delta_\sigma = \frac{4\pi e^2 \sigma_o^2}{3mc^2} \qquad (23)$$

If $\lambda_o \simeq 2265$ Å, $\sigma_o \simeq 44100$ cm^{-1} then the natural width in a wave-number scale for the components of the line under consideration in the present work, is approximately:

$$\delta_{2265\text{ Å}} \simeq 2.3 \text{ mk.} \qquad (24)$$

Quantum mechanically the natural breadth of a line arises from the finite lifetime of the atomic energy levels involved in the transition and the consequent uncertainty in the energy value. Weisskopf and Wigner[52] have calculated the natural line width assuming,(i) a Lorentzian distribution of the probability of the energy of a level, and (ii) Dirac's theory of the electron, and obtained the same results.

If the lower level in a transition is the ground state, which

is absolutely sharp, they found that the Lorentz profile, equation (20), remains valid, provided the classical quantity γ is replaced by the reciprocal of the mean lifetime given by quantum theory, but if the lower state is also unstable, the line is broader than the value given by that equation. In this latter case the parameter γ in the classical formula must be replaced not by the sum of transition probabilities from the upper level alone but by the sum of transition probabilities of all lines which start from either the upper or the lower state. The fact that a line is broadened by the existence of lines starting from its lower state, can be qualitatively deduced from the basic concepts of Dirac's theory, without calculations. The two terms E_1 and E_2 involved in a transition have finite energy widths ΔE_1 and ΔE_2. The intensity distribution has a half width determined by the half width of the involved terms. In wave-numbers:

$$\Delta\sigma = \frac{\Delta E_1}{hc} + \frac{\Delta E_2}{hc} . \qquad (25)$$

The half width if the terms E_1 and E_2 are connected to their mean lifetime t_1 and t_2 through the uncertainty relations: $\Delta E_1 . t_1 = \hbar$, $\Delta E_2 . t_2 = \hbar$, and t_1 and t_2 depend on all transition probabilities of the terms E_1 and E_2 respectively.

III - b) Doppler broadening

Here it is possible to distinguish between two effects, the

Doppler broadening produced by the random motion of the radiating atoms and that produced for other kinds of motions, as in the case of laboratory plasmas under certain circumstances. The present work is concerned only with the Doppler width produced by random motion as it is the only one which may be important in the atomic beam light source which was used in this work.

If an atom is moving with a linear velocity $\bar{v}$ relative to the observer, and emits light of frequency w_o, the frequency appears to be[22]:

$$w = \frac{w_o}{\sqrt{1 - v^2/c^2}} \cdot \left(1 - \frac{v}{c} \cos \theta\right) \qquad (26)$$

where:

θ is the angle of $\bar{v}$ relative to the direction of observation,

$v = |\bar{v}|$

w is the frequency as seen by the observer.

For light sources which are commonly used the random thermal motions are much smaller than the speed of light so that in equation (26), it is possible to expand $1/\sqrt{1 - v^2/c^2}$ in powers of v/c and keep only first order terms in this quantity. Then, equation (26) takes the approximate form

$$w' = w\left(1 - \frac{v}{c} \cos \theta\right) \qquad (27)$$

and the Doppler effect is appreciable only if the velocity $\bar{v}$ has a non-negligible component in the direction of observation.

According to the Maxwell distribution law, the probability that the component $u = v \cos \Theta$ lies between u and u + du is:

$$dp = (b/\pi)^{1/2} \cdot \exp.(-bu^2) \qquad (28)$$

where $b = M/2RT$, M is the molecular wight, R is the gas constant and T is the absolute temperature.

Then, replacing $u = (\cos \Theta) \cdot v$ as given in equation (27), in equation (28) and remembering that the intensity as a function of the frequency is proportional to the number of molecules having a given u component of the velocity one obtains

$$I(w) = \text{const.} \exp.\left[- bc^2 \frac{(w_o - w)^2}{w_o^2} \right]. \qquad (29)$$

From equation (29) the half-width is

$$\delta_D(w) = (\ln 2)^{1/2} \frac{w_o}{c} \, b^{-1/2} \qquad (30)$$

Equation (30) is valid as the half width line in emission and absorption when the natural width is considerably smaller than this Doppler width. The Doppler width for the present problem is estimated in the next chapter.

In equation (30) it is apparent that the Doppler broadening

is (i) proportional to the square root of the temperature, (ii) proportional to the frequency w_o, and (iii) proportional to the molecular weight to $-\frac{1}{2}$.

As a function of the wave-length equation (30) is

$$\delta_D(\lambda) = (\ln 2)^{\frac{1}{2}} \cdot \frac{\lambda}{c} \cdot b^{-\frac{1}{2}} \cdot \qquad (31)$$

While the natural width is constant in a wave-length scale, the Doppler width drecreases with the wave-length.

When the natural width is taken into account the intensity distribution as a function of the frequency due to the Doppler broadening is given by Weisskopf[53] as

$$I(w) = \frac{n}{\pi^{3/2} B} \int_{-\infty}^{+\infty} \frac{\exp.(-\Delta^2/B^2)\ d\Delta}{(w - w_o - \Delta)^2 + \delta_n^2} \qquad (32)$$

where:

$\Delta = uw/c$

δ_n is the natural width

w_o is the central frequency when only the natural width is taken into account, and

$$B = \frac{w_o}{cb^{\frac{1}{2}}} \cdot$$

III - c) Broadening caused by interactions between the radiating atom and its neighbors

Three cases may be distinguished, (i) Lorentz collision damping, (ii) the broadening and displacement of lines by force fields of neighboring atoms. There is a fundamental difference between the cases in which the neighboring atom is of a different kind than the radiating one, and, the case in which both atoms are identical. If both atoms are identical the broadening is called resonance broadening. If the atoms are different, the broadening is produced as a consequence of the sudden changes of phase of the radiation from the atom induced by collisions between the radiating atom and other atom in the gas. Weisskopf[53] considered this kind of broadening, assuming the classical model of Lorentz for the radiating atom while the collision process is considered from a quantum mechanical viewpoint. The Fourier analysis of the radiation undergoing such changes of phase yields a result of the same form as that found by Lorentz[33] and has the same kind of profile as the natural radiation. The half width depends upon the so-called collision damping constant which is equal to the inverse of the mean time between effective collisions. As the number of collisions between atoms in the atomic beam light source is

very small, this effect will not be considered here in detail.

Among the effects included in (ii) the Stark effect broadening is one of the most important. An electric field between the atoms is created by the charges, dipole moments and quadrupole moments of the atoms present when one of them is radiating. This broadening is very difficult to estimate. The variations of the intermolecular fields as a function of time are very complicated. Also there is some question as to whether the Stark effect which is obtained with fields varying considerably in both time and space are the same as would be obtained in constant fields. The assumption that the splittings of the term is determined by the field strengh at the center of the atom is due to Holtsmark (see for example Weisskopf[53]). In general it is assumed[54],[53] that the average field strength in the center of radiating atom is given by

$$F_o = C_1 e N^{2/3} + C_2 d N + C_3 Q N^{4/3}$$

where C_1, C_2 and C_3 are constants which must be calculated,

e is the charge of an ion,

N is the number of gas atoms per cm^3,

d is the dipole moment of an atom, and

Q is the quadrupole moment.

If the first order Stark effect is considered (linear Stark

effect) the broadening is symmetrical. The second order gives asymmetric broadening. In the first case the profile obtained is again Lorentzian.

In the present work no attempt was made to estimate the Stark broadening of the several components of the line under study but it is thought that it could be one of the causes that reduced the final resolving limit, as it is pointed out in chapter V. In order to excite the 2265 Å in Cd II a rather high excitation current as well as a rather high ion concentration is required.

The phenomenon of resonance broadening could also affect the line width of the hfs components. It is due to the interaction between an atom in a resonance state with an atom of the same kind in the ground state. Two different processes may be distinguished, namely an interaction by means of the induction field and an interaction by means of the radiation field. This second process may be considered as the emission of a photon produced by the excited atom and its absorption by another atom in its ground stafe. This latter process is the one that could be important in the atomic beam. Actual collisions in an atomic beam are rare events and do not then contribute to line broadening.

The emission and reabsorption of a photon gives rise to the common phenomenon of self absorption. This is most likely to occur when the concentration of the atoms (ions in the case considered here) in the ground state is high. The re-absorption is stronger for the more intense parts of the profile, so that the top of the line profile tends to be flattened, which yields an apparent broadening of the line. To avoid such effect the density in the beam must not be too high.

In some photographic plates, with the density in the beam used in the experiment, the singlet resonance line 2288 Å of Cd I not only was broadened by self-absorption, but sef-reversal made the line appear as two components. The concentration of singly ionized cadmium atoms is always much lower than the concentration of neutral atoms and therefore this effect of self-absorption is not as pronounced for the Cd 2265 Å as it is for the Cd I 2288 Å transition. No indication whatever of self-reversal was observed for 2265 Å but there may have been some broadening of the components due to this effect.

Chapter IV

LIGHT SOURCE

The line 2265 Å ($5s\ ^2S_{1/2} - 5p\ ^2P_{1/2}$) in cadmium II was excited in an atomic beam light source shown schematically in fig. IV - 1). In fig. IV - 2) a photograph of the atomic beam is shown. Its characteristics are similar to those described by Crawford et al.[11] and it is the same as the one used by Tomchuk[50] to study the hfs of the 2288 Å line in Cd I. This time the atomic beam was started when a pressure of 10^{-5} mm of Hg in the vacuum chamber was reached. The steel furnace was coated with Saureisen cement in which a winding of a nickel-chrome resistence wire was embedded. The total resistence at room temperature ranged from 9 to 20 ohms and the necessary temperature was maintained by applying different voltages to the furnace.

The electron gun consists of several light-bulb or fluorescent lamp filaments connected in parallel and coated with a triple carbonate powder suspended in an amyl acetate solution of nitro-cellulose intended primarily for spray application. The carbonate consisted of 49 % $BaCO_3$; 44 % $SrCO_3$ and 7 % $CaCO_3$ by weight, and it was provided by the Bell Telephone Laboratories.

It is necessary to bake a new furnace thoroughly because the gases released by the cement poison the emission coating material of the filament, and quench the anode current in a short time.

For baking, the working voltage was applied to the empty furnace, kept under vacuum for several hours.

Operating conditions were fixed according to the intensity shown in the photographs by the 2265 Å. The most significant quantities proved to be the anode current and the difference in voltage between grid and anode. Unfortunately both quantities had to be rather high (about 400 mA and 300 V respectively) to excite the Cd II line. When one of these two values was not so high only the 2288 Å of Cd I was shown in the photograph. This high anode current may produce an ions concentration which is too high and hence a possible Stark broadening in the components to be measured, (see chapter III).

The light produced in the atomic beam was observed at right angles to its long axis so that the effective velocity components in the line of sight is considerably reduced. In this way the Doppler broadening (see chapter III) is much smaller than that expected from the temperature of the atoms. A schematic drawing of the atomic beam is shown in fig. IV - 3). The paths of the atoms are limited to the dotted lines defined by the slits. The furnace aperture is a hole 2 mm in diameter at the center of the iron cap of the furnace.

Assuming that the aperture of the furnace a (see fig. IV - 3)

is much smaller than s, the upper slit length, Tolansky[49] indicates that the half width of the intensity in terms of the frequency in the atomic beam due to Doppler broadening is only appreciably affected by the values s and h, where h is the distance between slits. If w_b is the half width of a line in the beam and w_f is the half width of the same line due to Doppler broadening at the temperature of the furnace, Tolansky's calculation yields

$$w_b = 0.41 \frac{s}{h} w_f \qquad (1)$$

The Doppler width in the furnace is given by (see chapter III)

$$w_f = \frac{2\sigma_o}{c}\sqrt{\frac{2RT \ln 2}{M}} = 7.16 \times 10^{-7}\ \sigma_o\sqrt{T/M}$$

where T is the absolute temperature, and M the molecular weight. For the 2265 Å line in Cd II in the experimental conditions under consideration, one has $M \simeq 110$, $T \simeq 700$, $\sigma_o \simeq 44000\ cm^{-1}$. Then, $w_f \simeq 78$ mk and the Doppler half width of the beam is approximately

$$w_b \simeq 32\ s/h\ mk$$

As the ratio s/h is smaller than 0.1 the Doppler width is near 3 mk, which is of the same order of magnitude as the natural breadth (see chapter III). Therefore this method of calculating the Doppler width is not very accurate, though a rough order of magnitude can be obtained.

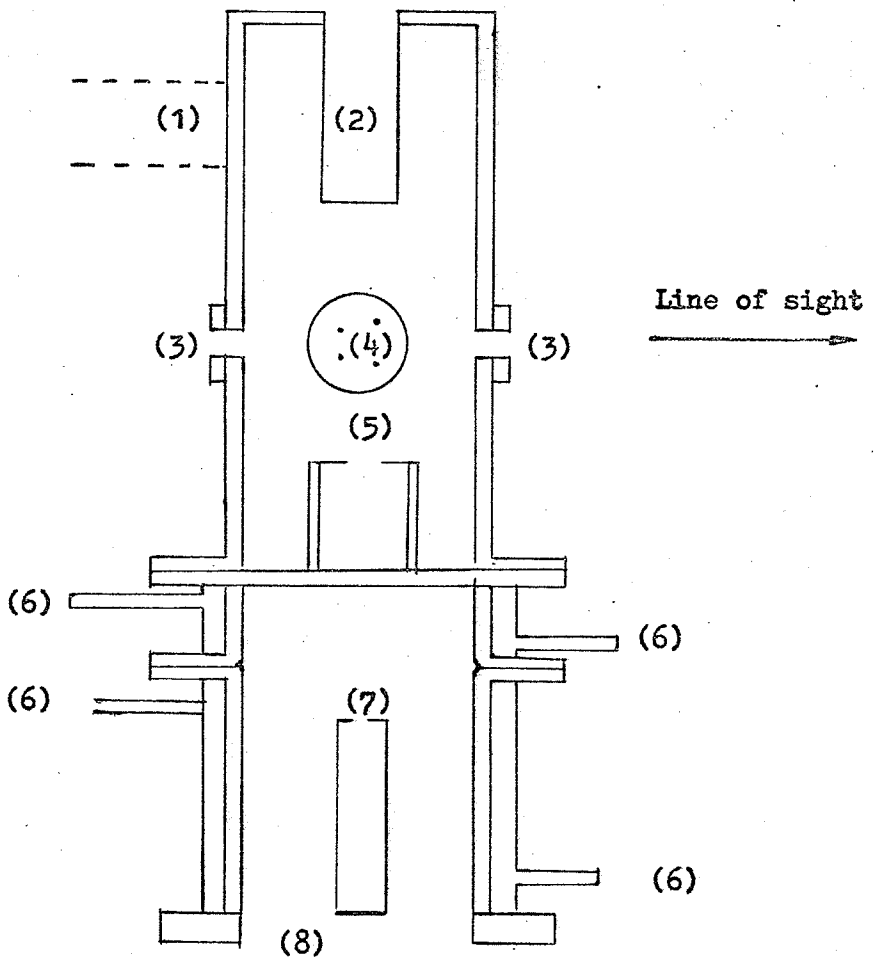

Fig. IV - 1): Atomic beam light source. (1) to pump; (2) liquid N_2 trap; (3) windows; (4) filament and grid of the electron gun; (5) upper slit; (6) cooling water; (7) furnace with a lid with a hole 2 mm in diameter which provided the lower slit; and (8) to pump.

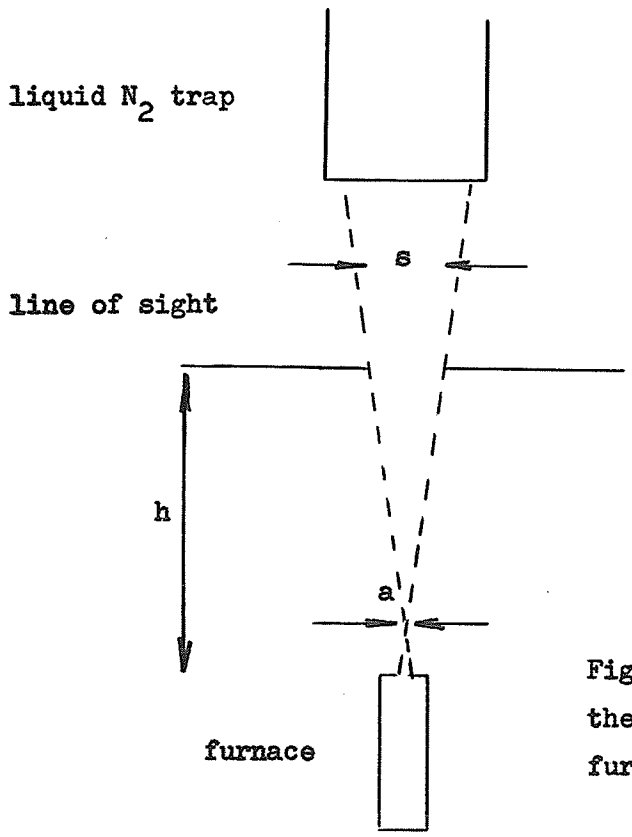

Fig. IV - 3) Schematic drawing of the atomic beam coming from the furnace.-

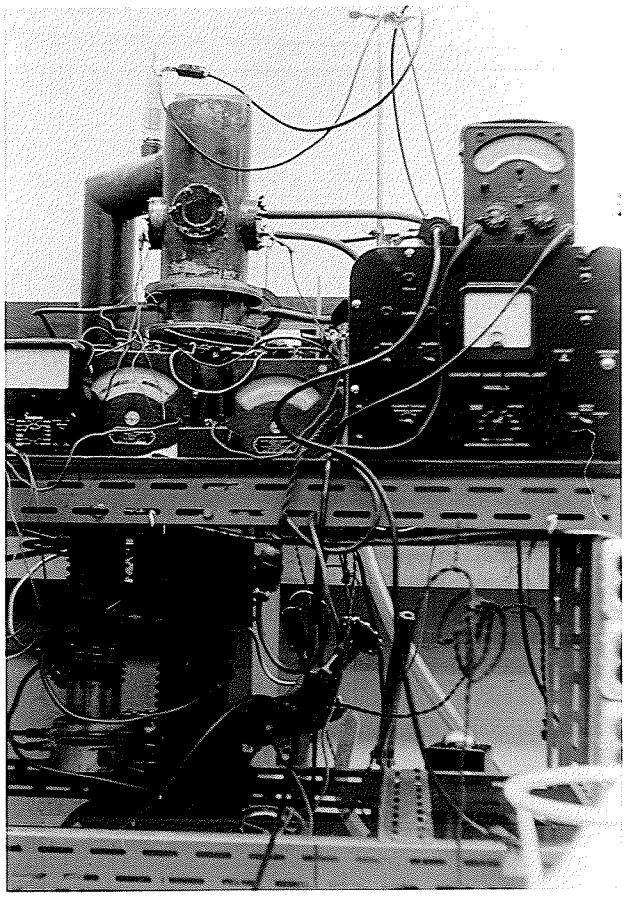

Fig. IV - 2) Photograph showing the atomic beam light source. At the background it is possible to see the quartz lens which concentrated the light coming from the source on the Fabry-Perot.-

Chapter V

OPTICAL SYSTEM

To obtain high resolution a Fabry-Perot interferometer crossed with a Hilger Medium Quartz Spectrograph (f/10) was used. The interferometer consists of two transparent plates each of them having a face, in principle, perfectly plane. These plates are covered with a reflecting coating of reflection coefficient R, transmission coefficient T, and absorption coefficient A. These coefficients are connected by $R + T + A = 1$. The plates are set up with the coated faces parallel to each other. The theory of the Fabry-Perot interferometer is discussed in quite a few books and papers. The short introduction here follows the references under the numbers (35), (49),(23) and (3).

When the plates are illuminated with a monochromatic and parallel beam, the transmitted rays interfere since they are split off from one original wave (i.e. they are coherent). The interference patterns are sharp at infinity or in the focal plane of a lens if the rays are let to pass through it. The phase difference that two consecutive rays have at infinity is given by

$$\text{phase difference} = 2\pi (2t \cos \phi/\lambda) \qquad (1)$$

where t is the distance between the two plates,

ϕ is the incidence angle of the rays illuminating the first plate,

and λ is the wavelength of the radiation in the medium

between the two plates.

The factor in brackets in equation (1) is called the order number and it is usually designed by p,

$$p = \text{the order number} = \frac{2t \cos \phi}{\lambda} = 2t \sigma \cos \phi \qquad (2)$$

where σ is the wavenumber in the space region where the wavelength is λ.

When the phase difference given by (1) is an even multiple of π the emerging beams produce constructive interference and hence a maximun of intensity.

When this difference is an odd multiple of π, destructive interference is produced and therefore a minimun of intensity.

According to equation (2), this is the same as saying that the maxima of intensity correspond to integral values of p. The interference patterns are circles whose radii depend on the incidence angle ϕ and whose diameters are related to p according to the following approximate equation[35]

$$p \cong 2t \sigma \left(1 - \frac{D^2}{8f^2}\right) \qquad (3)$$

where D is the diameter of the ring corresponding to p, and f is the focal distance of the projecting system.

Equation (3), upon differentiation, shows that for equal

increments of p there will correspond equal increments in D^2, i.e., the difference between the D^2 of consecutive circles is constant, and is given by

$$\Delta(D^2) = \frac{D_k^2 - D_i^2}{k - i} = \frac{4f^2}{\sigma t} \qquad (4)$$

where D_k is the diameter of the k'th ring, D_i that of the i'th one.

To use the Fabry-Perot interferometer to measure the separation between two close components it is necessary to consider the order of the center, P, which is defined putting D = 0 in equation (3) or $\phi = 0$ in equation (2), that is to say, $P = 2t\sigma$. This also may be expressed as the integral order of the first bright ring p_o plus a positive fractional part e, where $P = p_o + e$. This equation is the definition of e. It may be shown that

$$e = \frac{D_i^2}{\Delta(D^2)} - i \qquad (5)$$

where D_i is the diameter of the i'th ring. Then the separation in wave-numbers of two close components is

$$\sigma_1 - \sigma_2 = \frac{p_1 - p_2}{2t} + \frac{e_1 - e_2}{2t} \qquad (6)$$

where the indices 1 and 2 refer to the two components.

If the orders do not overlap, i.e. the difference $\sigma_1 - \sigma_2$

is smaller than the "spectral range" (see below) then the difference $p_1 - p_2$ is zero. Otherwise it is necessary to use different spacers (etalons) to decide its value.

The spectral range is defined as the change in wave-number necessary to shift the ring system by the distance of consecutive orders. The value of the spectral range may be found from equation (2), putting

$$(p + 1)\lambda_1 = p\lambda_2$$

that is to say, the λ_2 ring of order p is in coincidence with the λ_1 ring of order $(p + 1)$. Then,

$$\text{spectral range} = \Delta\lambda = \frac{\lambda^2}{2t}$$

or in terms of the wavenumber,

$$\text{spectral range} = \Delta\sigma = \frac{1}{2t} \qquad (7)$$

where t is the length of the etalon gap.

Here also should be noted that from equations (2) and (3) it is apparent that σ increases outwards the center of the rings, while p and λ increase towards the center of the rings (see fig. V - 1).

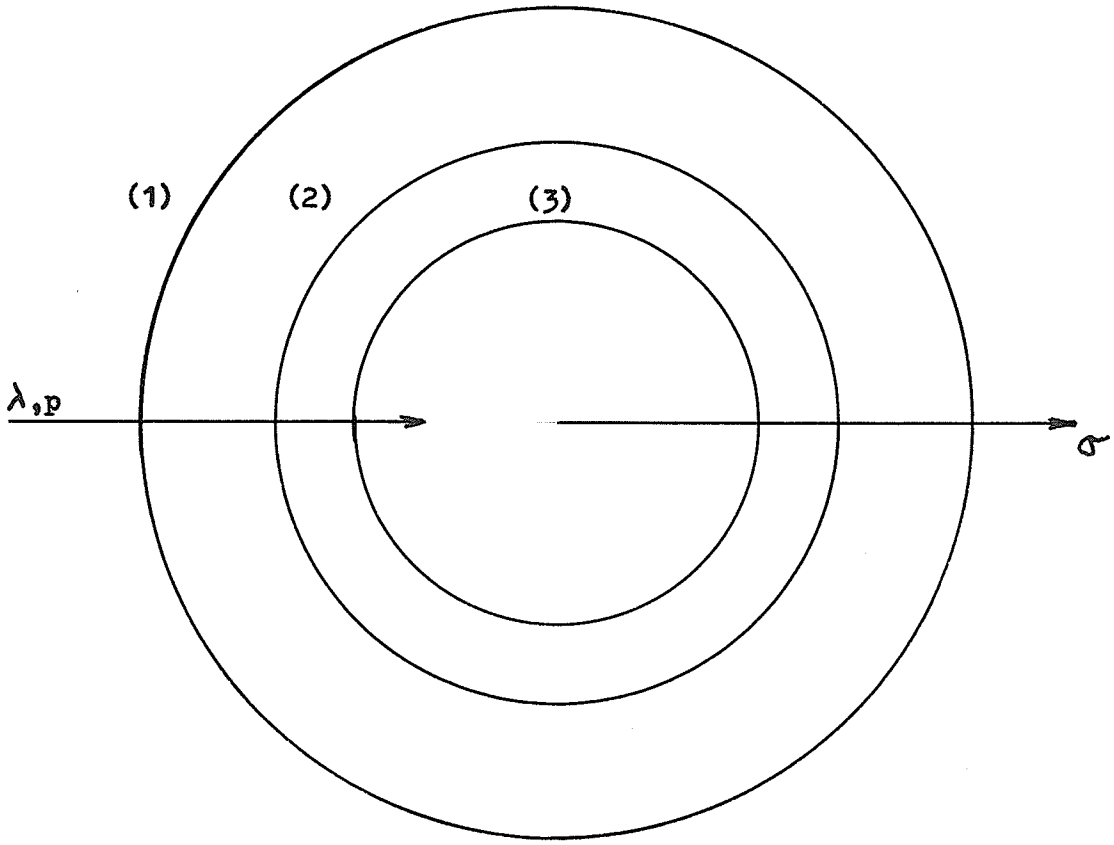

Fig. V - 1) Schematic drawing showing the interference pattern produced by the Fabry-Perot interferometer when there are two close components, with wavelengths λ_a and λ_b. (1): ring of order p produced by the component of wavelength λ_a; (2): ring of order p produced by the component of wavelength λ_b; and (3): ring of order p + 1 produced by the component of wavelength λ_a.-

V - a) Intensity distribution, resolving power and resolving limit

Adding the amplitudes of the reflected rays from the two reflecting surfaces and assuming that an infinitely fine line is incident upon the Fabry-Perot, it can be shown that the intensity distribution of the interference pattern is given by:

$$I = \frac{T^2}{(1-R)^2} \times \frac{1}{1 + \frac{4R \sin^2(\pi p)}{(1-R)^2}} \times I_o, \qquad (8)$$

where all symbols have the same meaning as before, and I_o stands for the incident intensity.

The maxima of this expression occur when p is an integer, as it was pointed out before. Then,

$$I_{max} = \frac{T^2}{(1-R)^2} \times I_o \qquad (9)$$

If the mirror surfaces are ideal, the absorption coefficient A = 0, and $I_{max} = I_o$, the fringes have the same intensity as would be obtained without the Fabry-Perot interferometer.

The minima occur when p is equal to an integer plus one half,

$$I_{min} = \frac{T^2}{(1 + R)^2} \times I_o \qquad (10)$$

Along a diameter of the ring system the intensity fluctuates between the values given by equations (9) and (10).

The intensity at half-width, defined as the change in wave-number necessary to reduce the intensity to one half of its maximun value, has the approximate expression

$$2\sigma_h = \frac{(1 - R)}{\pi \sqrt{R}} \qquad (11)$$

which gives a measure of the sharpness of the fringes.

The apparatus width may be defined as the intensity half-width times the spectral range

$$a = 2\sigma_h \cdot \Delta\sigma = \frac{\Delta\sigma}{N_R} \qquad (12)$$

where $N_R = \frac{R}{(1 - R)}$ is called the "reflecting finesse" and depends only on the reflection coefficient R.

The resolving power of the Fabry-Perot is defined by the equation

$r = \lambda/\Delta\lambda$, where $\Delta\lambda$ is the wavelength difference of two monochromatic lines of equal intensity which can be seen just separated by the interferometer. To give a meaning to "just separated" the Rayleigh criterion is generally used. According to this condition the two lines of equal intensity are said to be resolved if their maxima of intensity and the minimun intensity between them have the ratio $1 : 0.8106 \simeq 1 : 0.8$. In this way an approximate value of the resolving power is given by:

$$r = p\, N_R \qquad (13)$$

The resolving power also may be written in terms of the difference in wave-number corresponding to λ and $\Delta\lambda$, $\lambda/\Delta\lambda = -\sigma/\Delta\sigma$, or $|\Delta\sigma| = \sigma/r$. This quantity is called by Tolansky[49] "the resolving limit of the instrument".

In the results given above it was assumed that the plates were perfectly plane and parallel, and that the grain size of the plates used to record the interference patterns is negligible. The actual conditions produce a departure in the intensity distribution as given by equation (8) and make a further limitation on the resolving power of the instrument. This may be taken into account introducing two new "finesse" parameters, namely, the "limiting finesse" N_d and the "photographic finesse" N_p. The first one is due to departures from flatness in the mirrors, whether they would be produced by faults of micro-smoothness, by curvature of the plates or by lack of adjustement

(parallelism); and the second one is due to the resolving limit of the photographic emulsions used to record the interference patterns. The last one, under ordinary conditions, may be neglected (i.e. it may be assumed that $N_p = \infty$).

The "limiting finesse" has the expression $N_d = \frac{1}{2} m$ where m is in the cases cited above: i) faults of micro-smoothness following a Gaussian distribution whose half-width is λ/m; ii) spherical curvature of the plates defined by its sagitta whose value is λ/m; and iii) a distance between plates which is $t \pm \lambda/m$.

The resultant resolving limit may be described by the "effective finesse" of the Fabry-Perot, in analogy with equation (12)

$$a_{th} = \frac{\Delta\sigma}{N} \qquad (14)$$

where N is the "effective finesse", and th stands for "theoretical", meaning that this resolving limit only takes into account the factors cited above.

A plot of N/N_d vs. N_R/N_d is reproduced in Dickie's Ms of Sci. Thesis[13].

V - b) Influence of the dispersion of air

The dispersion of the air must be taken into account. On one hand changes in temperature and pressure between the plates of the interferometer affect its resolving limit, and on the other hand, although the relative values of wave-numbers are affected only slightly by the variation of the air conditions, when measuring small wave-number differences, the corrections cannot be neglected in accurate measurements.

When temperature and presure between the two interferometer's plates are not kept constant, the optical length nt changes. n is the refractive index of the air between the plates and t is the plates' separation. Therefore, the phase difference between two consecutive rays as given by equation (1) is not a constant if the atmospheric conditions change. The change in the refractive index of the air as a function of the temperature and pressure is given by Edlén's formula (see Svensson[48])

$$\Delta n = n - n_s = (n_s - 1)\left(\frac{d}{d_s} - 1\right) \qquad (15)$$

where, n is the refractive index of the air at pressure P and temperature T,

n_s is the refractive index of standard air. Standard air is, by definition, dry air containing 0.03 per cent by volume of CO_2, at normal pressure (760 mm Hg at 0°C and g = 980.665 cm/sec^2)

and a temperature of 15°C. n_s as a function of the wave-number σ is given by[48]

$$(n_s - 1) \times 10^8 = 6{,}432.8 + \frac{2{,}949{,}810}{146 - \sigma^2} + \frac{25{,}540}{41 - \sigma^2}, \qquad (16)$$

d is the density of the air at pressure P and temperature T,

d_s is the density of the standard air.

The dependence of d with pressure and temperature is given by[48]

$$\frac{d}{d_s} = \frac{P(1 + 15\alpha)(1 + \beta P)}{760(1 + \alpha T)(1 + 760\beta)} \qquad (17)$$

where,

$$\alpha = 0.003674\ (°C)^{-1}$$

$$\beta = 0.73 \times 10^{-6}\ (\text{mm Hg})^{-1}$$

In table I some values of the factor $(\frac{d}{d_s} - 1)$[48] as a function of T and P are reproduced.

To reduce to vacuum conditions the difference in wave-numbers given by equation (6) it should be remembered that

$$\sigma_1 = \sigma_{1v} n$$

$$\sigma_2 = \sigma_{2v} n$$

where the sub-index v stands for vacuum conditions.

Then equations (6) becomes

$$\sigma_{1v} - \sigma_{2v} = \left(\frac{p_1 - p_2}{2t} + \frac{e_1 - e_2}{2t}\right) \frac{1}{n}$$

T A B L E I

P (in mm Hg)	24°C	25°C	26°C	27°C
730	-0.0687	-0.0718	-0.0749	-0.0780
740	-0.0559	-0.0591	-0.0622	-0.0654
750	-0.0431	-0.0464	-0.0496	-0.0527
760	-0.0304	-0.0336	-0.0369	-0.0401
770	-0.0176	-0.0209	-0.0242	-0.0275
780	-0.0049	-0.0082	-0.0116	-0.0149

Values of the factor $\left(\frac{d}{d_s} - 1\right)$ found by Svensson[48] are reproduced in this table as a function of temperature and pressure.

V - c) Experimental arrangement

To prepare the mirrors of the Fabry-Perot, two quartz plates polished to $\lambda/150$ were coated by evaporation with thin aluminium films. This kind of coating was chosen since the wavelength region of interest in the present work is located in the far ultra violet at 2265 Å. The evaporation was performed in a chamber described by Sutherland[47] and shown in fig. V - 2. Spectroscopically pure aluminium was used.

Periodically, as the coatings deteriorate with time, the quartz plates were cleaned and new aluminium films deposited. To remove the old aluminium concentrated HCl together with HNO_3 were used. After the aluminium was removed, the plates were thouroughly washed with detergent and after rinsed with distilled water and dried with clean lens paper. During the preparation of the film the pressure in the evaporator was lower than 5×10^{-5} mm Hg. The evaporation time was initially chosen from a graph of transmission vs. time of evaporation at a given voltage applied to the filament and a fixed amount of Al on the filament, but, for the trnasmissions required in these experiments this procedure proved to be not applicable. From the plot of transmission coefficient versus time it was concluded that 4.2 sec. was the correct time of evaporation. However, the transmission coefficient which was obtained in practice depended on non-controllable factors and transmission coefficients ranging from 0.002 to 0.07 were obtained with this constant time of evaporation. The transmission coefficients were measured in the blue region of the spectrum using a white light source, a commercial light meter combined with a blue filter. Since the transmission coefficient could not be accurately predicted in advance it was necessary to make several trials keeping all factors constant. When a transmission coefficient near 0.01 (in the region mentioned above) was obtained on both plates, the trials were stopped. In this way transmission coefficients ranging from 0.007 to 0,012 were obtained and used. When new coatings were needed, the transmission coefficient

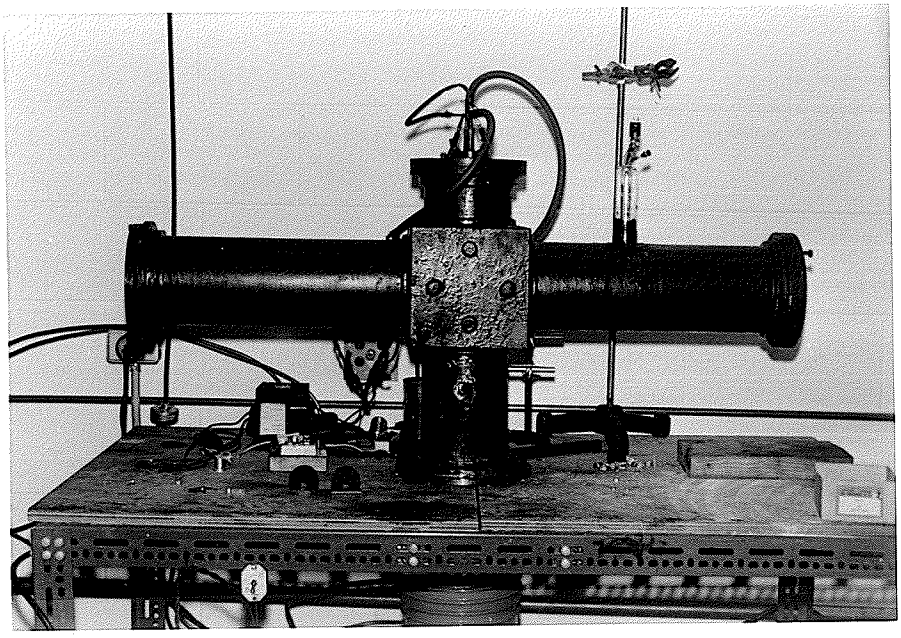

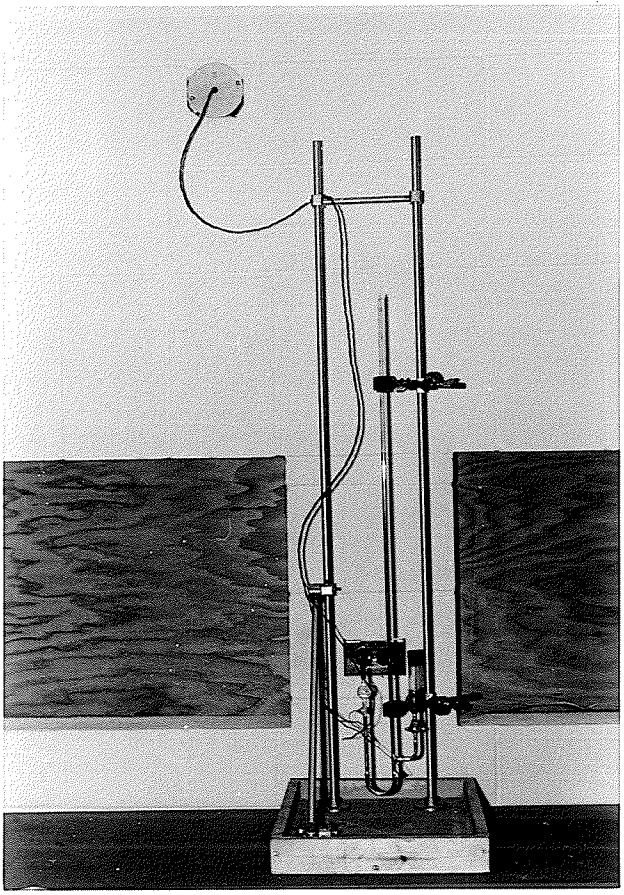

Fig. V - 2) Photograph showing the evaporation chamber used to coat the Fabry-Perot plates. It was described by Sutherland[47].

Fig. V - 3) Photograph showing the ether-mercury thermostat, described by Green and Loring, Rev. Sci. Inst., 11, 41, (1940), used to control the temperature in the spectrograph and interferometer room.

of the old films were measured again just before cleaning. In general values about twice as high as those found immediately after depositing the films were recorded. Short times of evaporation, which made conditions uncontrollable, were chosen as the reports of various observers agree that slow deposition of aluminium films produces low reflectivity. This phenomenon is explained by Burridge et al.[6] as due to the influence of the residual gases during the deposition of the film. These authors consider that the product of the time of deposition and the pressure in the evaporator is a significant parameter in terms of which to describe the optical properties of the thin aluminium films. In their work[6] they have measured the transmission and reflection coefficients of thin aluminium films deposited on silica in the spectral range between 4200 and 2600 Å and they extended by an indirect method the measure of R to wavelengths as short as 2300 Å. Using the direct method they made plots of (i) the relative transmission as compared with that at 3600 Å as a function of λ, ii) the sum R + T as a function of T using different values of the parameter pt (pressure times time of deposition) for the wavelengths 4200, 3600, 3200 and 2600 Å. Using the indirect method they measured reflectivites in 2400 and 2300 Å but they do not specify the transmission of these films in the blue region. That is why it is so surprising to read in Tomchuk's thesis[50]:..."from the curves of Burridge et al.[6] the reflection coefficient R could be determined for a particular wavelength in the ultraviolet"... and in Sutherland's thesis[47]:

... "(Burridge et al.[6] have shown that under optimun conditions) values of R + T = 0.90 can be obtained. With these plates a resolving power of 1/18 of an order was obtained without excessive loss of intensity"... . It should be noted that in the former work[50] the hfs of 2288 Å in Cd I was studied and in the latter one[47], the hfs of the lines 2144 and 2265 Å in Cd II were investigated.

Assuming that the tendency shown in the graphs given by Burridge et al.[6] is followed down to 2265 Å, a transmission coefficient of 0.01 in a wavelength near 4500 Å would correspond to a transmission coefficient of approximately 0.04 at 2265 Å. This in turn would give a sum R + T near 0.85. Whence the reflectivity at 2265 Å would hardly be expected to be higher than 0.81. A reflection coefficient of this value yields a "reflecting finesse" near 15, and, according to the specified quality of the plates, the "limiting finesse" cannot exceed 30. Using the plot of N/N_d versus N_R/N_d reproduced in Dickie's Master of Science's degree thesis[13] it is found that

$$N/N_d \cong 0.5 \qquad (18)$$

that is to say, $N \cong 15$. Using equation (14) to find the resolving limit it is found that for the 2 cm spacer, the spectral range is $\Delta\sigma = 0.250\ cm^{-1}$ and the resolving limit is approximately $a_{th} \cong 0.017\ cm^{-1}$. While for the 5 cm spacer, the spectral range is $\Delta\sigma = 0.100\ cm^{-1}$ and whence $a_{th} \cong 0.007\ cm^{-1}$.

In practice such low resolving limits were not obtained. Eq. (18) does not take into account the finite resolving limit of the photographic emulsion used. It was particularly important when medium grain Ilford Q.2 plates were used. With the fine grain Ilford Q.1 plates the resolving limit of the emulsion was much lower but the sensitivity was also much lower and considerably longer exposure times were required and the resolving limit deteriorated as a consequence of the changing atmospheric conditions and of the level of vibrations in the building which was considered to be rather high. The width of the spectral line also affected the resolving limit. As pointed out in chapter IV, the Doppler width is low since the emiting atoms have only a small component of velocity in the direction of observation. But, Stark broadening may have had a non-negligible effect since the ions field may have been rather high. The anode current used to excite the atomic beam could not be diminished as a low current did not excite the spectrum of ionized cadmium. No estimate of the width produced by Stark broadening could be made.

To minimize the effects of temperature and pressure changes on the resolving limit the interferometer and the spectrograph were set up in a temperature controlled room connected with the light source room through a slot in the wall. Fig. V - 3 shows the ether-mercury thermostat used to control the temperature which was kept approximately constant at 78°F (i.e. about 25.5°C). The temperature of the light

source room remained almost constant at 72°F (i.e. at 22.2°C). Unfortunately, there was a draft through the slot which allowed the passage of the light from one room to the other one. Besides, two of the heaters in the constant temperature room activated by the thermostat were under the interferometer and produced a further draft. Changes of the temperature of the air in the interferometer may have been the cause of some unsuccesful exposures.

To make an estimate of the allowable changes in temperature and pressure, equation (1) may be written as

$$\text{phase difference} = 2\pi(2t\sigma_v n)$$

where σ_v stands for the wavenumber in vacuum. This equation can be thought of as a function of n with σ_v constant. The phase difference corresponding to the "spectral range" is 2π (i.e. $\Delta p = 1$). Hence a change in the refractive index of air which gives a shift of a fringe in one order is: $2t\sigma_v n = 1$ or $\Delta n = 1/2t\sigma_v$ and the change of the refractive index which yields a shift in a ring equal to the resolving limit is

$$\Delta n = \frac{1}{2t\sigma_v N} \qquad (19)$$

where, as before, N is the "effective finesse". When $\lambda \cong 2265$ Å, $\sigma_v \cong 44100\ \text{cm}^{-1}$ equation (19) yields:

for $t = 2$ cm, $\quad \Delta n \cong 3.8 \times 10^{-7}$ (20)

for $t = 5$ cm, $\quad \Delta n \simeq 1.5 \times 10^{-7}$ (21)

Equations (20) and (21) show the change in the refractive index of the air necessary to shift a ring an amount equal to the resolving limit. The change in the refractive index of air due to a change in temperature and pressure is given by equation (15). The factor $(n_s - 1)$ according to Edlén's formula, is given by Svensson[48] for some wavelengths. From there, as an estimate, it may be considered that $(n_s - 1) = 3.09 \times 10^{-4}$. In table I values for $(\frac{d}{d_s} - 1)$ as a function of temperature and pressure are given. Assuming the pressure is kept constant at 760 mm Hg a change in temperature from 26 to 25°C (that is to say, a constancy in temperature in $\pm$ ½°C) would give a change in the refractive index of air of

$$\delta_n = (0.0369 - 0.0336) \times 3.09 \times 10^{-4} \simeq 10^{-6} \qquad (22)$$

a value which is about 2.5 times the one given in equation (20) and about 6 times as high as the one given in equation (21).

Table I gives values of the density factor each 10 mm Hg but considering a constant temperature of 25°C the change in the density factor is an almost linear function of the pressure. Then the effect on the refractive index of the air produced by a change in

pressure of 1 mm Hg is approximately:

$$-1.3 \times 10^{-3} \times 3.09 \times 10^{-4} \simeq -4 \times 10^{-7} \simeq \delta_n \qquad (23)$$

which is a bit larger than the value given in equation (20) and about 2.5 times the one given in equation (21).

From equations (22) and (23) it is clear that the resolving limit is not as low as it would be expected from the theoretical result (i.e. a_{th} = 17 mk for the 2 cm spacer and a_{th} = 7 mk for the 5 cm spacer).

From equation (22) and a_{th} = 17 mk for the 2 cm spacer, it is found that a change in $\pm$ ½°C produces a shift in a ring of about 40 mk, provided the pressure is kept constant at 760 mm Hg. And a change in pressure in $\pm$ ½ mm Hg produces, according to equation (23) and a_{th} = 17 mk, a shift near 18 mk, provided the temperature is kept constant at 25°C. The same shifts in mk are produced using any other spacer. The difference is the fraction of the spectral range covered with different spacers.

At the start of the experiments the interferometer was enclosed in an evacuated chamber with two quartz windows. As it was not possible to rely on the constancy of the pressure inside such chamber, it was taken out and the exposure times were considerable shortened since there was no loss of intensity in the windows. However, the best plates

obtained were taken with the vacuum chamber.

The plates of the Fabry-Perot and the whole optical system are made from fused quartz because the line intended to be measure is located in the far ultraviolet. The plates of the Fabry-Perot are slightly prismatic. The two surfaces of each one make an angle of several minutes with each other. The coated faces of the two plates were kept in a parallel position by a spacer of fused silica. To set up the interferometer the optical contact between the faces of the plates and the spacer was checked by the Newton's rings formed when the plates were slightly pressed against the pins of the spacer. After that, the parallelism of the plates was adjusted by observing through a telescope of small aperture the fringes of the mercury green line produced in a water-cooled mercury ^{198} lamp. As the light source was not an extended one, but a linear one, to adjust the interferometer, the fringes were observed using two different positions of the mercury lamp, perpendicular to each other. As the coatings of the plates were too thick to permit the measurement of the diameter of the rings using a scale in the telescope, a ring system was observed in which a bright ring just began to emerge from the center. The change of the intensity distribution of this spot could be judged with high accuracy.

One quartz lens, mounted between the source and the Fabry-Perot interferometer, served to produce a parallel beam of light from the source and incident on the Fabry-Perot. A second good quality lens was mounted following the Fabry-Perot and served to focus the ring system on the slit of the spectrograph. The experimental positions of the lenses are given by Tomchuk[50].

In fig. V - 4, a photograph of the Hilger Medium Quartz Spectrograph used in this work is shown, while in fig. V - 5, a photograph of the mounting and spacer of the Fabry-Perot interferometer are shown.

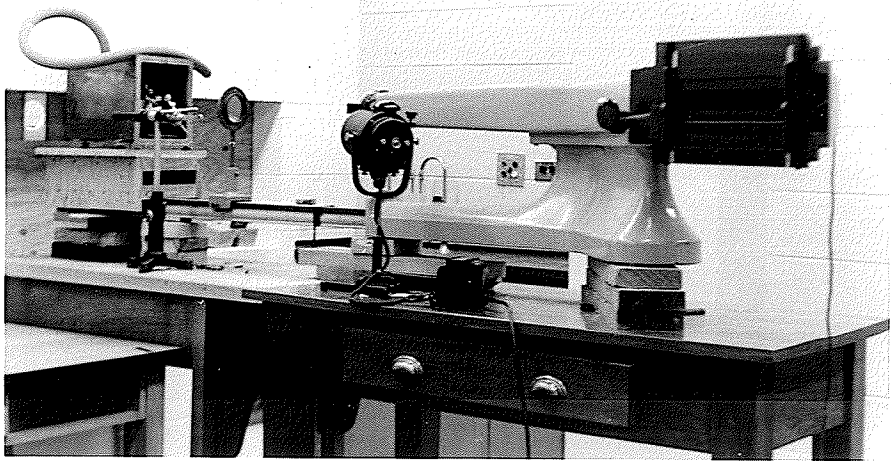

Fig. V - 4) Photograph showing the Hilger Medium Quartz Spectrograph which was used to cross the Fabry-Perot interferometer.

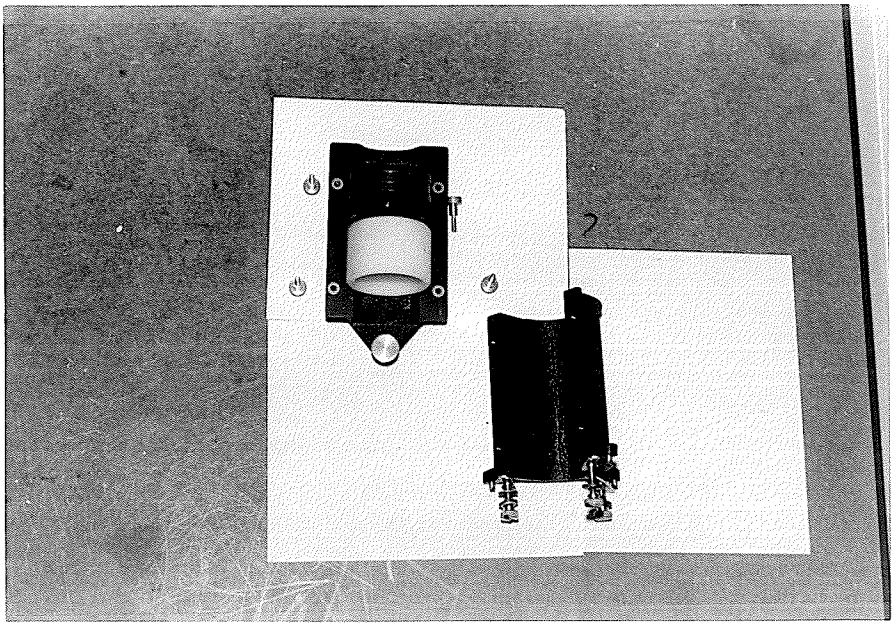

Fig. V - 5) Photograph showing the Hilger mounting and spacer of the Fabry-Perot interferometer.

Chapter VI

EXPERIMENTAL RESULTS

To measure the hyperfine structure of the transition 2265 Å ($5s\ ^2S_{1/2} - 5p\ ^2P_{1/2}$) in Cd II, spacers of 2 and 5 cm in the Fabry-Perot interferometer were used. The interference patterns were recorded in Ilford Q.1 and Q.2 photographic plates. The exposure times ranged from 2 to 9 hours. Heavier coatings on the Fabry-Perot plates require exposure times longer than 9 hours. However, in 9 hours the furnace of the source is exhausted. To refill the furnace it is necessary to disassemble the vacuum chamber and after that to make a realignement of the source which made it impossible to continue the same exposure. A very long exposure time with fine grain Q.1 plates and low transmission in the Fabry-Perot mirrors proved to be no more useful than a relatively short one with medium grain Q.2 plates or with Q.1 plates with higher transmission in the Fabry-Perot mirrors. As discussed in chapter V the reason for this is assumed to be the uncontrollable atmospheric conditions as well as the high level of vibrations in the building. Another adventage of short exposure times is the use of the same charge of cadmium in the furnace of the source to take several exposures and in this way to make corrections for small misalignements. Each time the furnace is refilled the atomic beam light source must be taken apart and after reassembly it is necessary to make a careful realignement as the conditions are such that it is not possible to be certain of

maintaining precisely the same position for the radiating atoms of the beam. The entire procedure for recharging the furnace and realignement of the source takes most of a day. Ilford microphene developper was used to develop the plates.

When the 2 cm spacer is used the fringe pattern shows three components. One of them is much stronger and broader than the other two and is ascribed to the non-resolved components of the even isotopes. This broad component will be called the component 1 of the 2 cm spacer. The other two will be called the components 2 and 3 of this spacer. They are thought to be due to some of the magnetic hfs components of the odd isotopes.

A schematic view of the pattern obtained with the 2 cm spacer is shown in fig. VI - 1). The separations shown in this figure are the mean values of 13 independent measurements. The errors are the r.m.s. of the diviation from the average for the distribution.

With the 5 cm spacer, the fringe patterns again shows three components, though in some exposures a fourth one can be observed, as a faint fringe. This fourth component has been measured, and, the results are consistent but it is assumed that the probable error may be larger than the one given by the r.m.s. of the distribution. These components are called 1, 2, 3 and 4 of the 5 cm spacer. A schematic view of the pattern of the 5 cm spacer is shown in fig.VI-2).

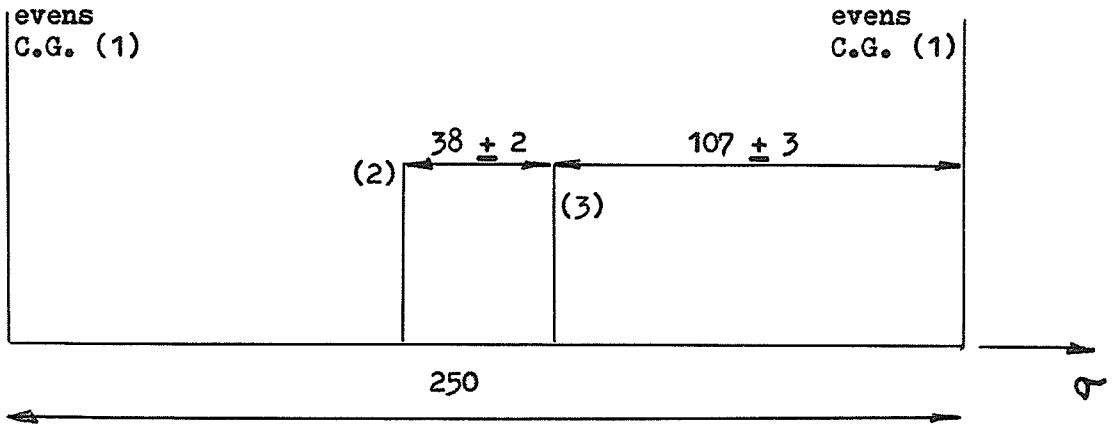

Fig. VI - 1) Schematic pattern displayed by photographic plates taken with the 2 cm spacer. Distances are given in mk. These values are the mean values of 13 independent measures. The errors are the r.m.s. of the distribution.-

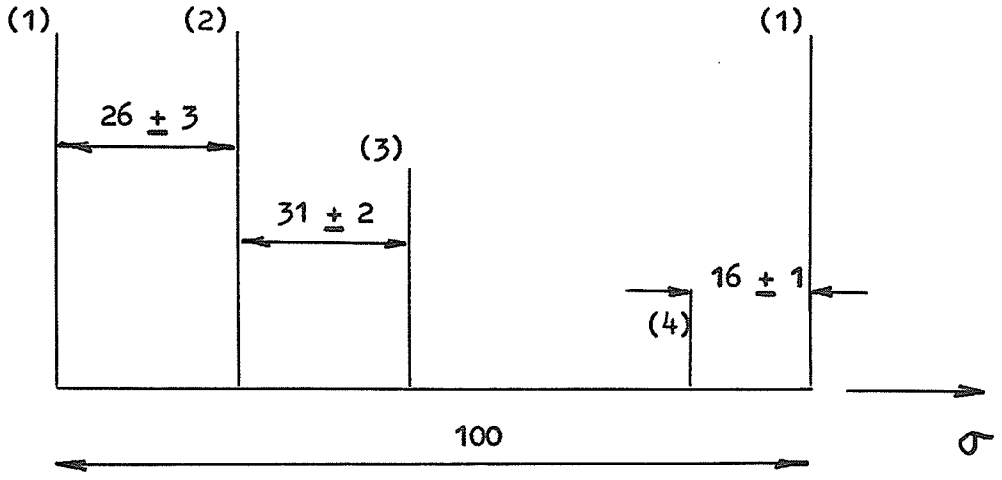

Fig.VI - 2) Schematic pattern found when using the 5 cm spacer. The di distances betwee the components (1) and (2), and (2) and (3) are the mean values of 19 independent measures from three different plates. The separation between components (4) and (1) is the mean value of 5 independent measures of 1 plate. The errors are the r.m.s. of the distributions. All distances are given in mk.-

To interpret the structure found with both spacers some assumption must be made. To begin with it is possible to compare fig. VI - 2) with fig. I - 3). Though there may be some alterations in the observed separations produced by the distribution of the components of the odd isotopes, a good assumption is to ascribe the component 1 with the 5 cm spacer to the component produced by the isotope of mass 114, component 2 to that produced by the isotope of mass 112, 3 to the isotope of mass 110 and 4 to the isotope of mass 116, although this component 4 belongs to different order of interference in fig. VI - 2). Some corrections will be made later to allow for the influence of the odd isotopes. The ratio between the separations of the even isotopes found here, and those shown in fig. I - 2) for the Cd I 3261 Å, are:

$$\frac{\Delta\sigma'_{114-112}}{\Delta\sigma_{114-112}} \simeq 1.9; \qquad \frac{\Delta\sigma'_{112-110}}{\Delta\sigma_{112-110}} \simeq 1.9$$

Then, in place of the factor 1.6 assumed in fig. I - 3), for the ratio of the isotope shifts in Cd I 3261 and Cd II 2265 Å, it seems more reasonable to use a factor of 1.9. When this is done the separation between the centers of gravity of the odd isotopes in 2265 Å is predicted to be

$$\Delta\sigma'_{111-113} = 1.9\,\Delta\sigma_{111-113} = 1.9 \times 17 \text{ mk} \simeq 32 \text{ mk} \qquad (1)$$

As the two odd isotopes have different magnetic moment (see chapter I) the components a^{111} and a^{113}, etc. are not separated by the amount

shown in equation (1). To estimate these separations the nuclear magnetic moments listed by Mack[34] are used. The values of the nuclear moments are: -0.5949 n.m. for Cd^{111} and - 0.6224 n.m. for Cd^{113}.

An estimate of the splitting of the terms 5s and $5p_{1/2}$ in Cd II can be obtained using equations (3.7) and (3.9) of Sutherland's thesis[47] (equations (1) and (2) chapter I of this thesis) which gives:

$$a(5s) = 0.4186\ g(I) = 0.4186 \times 2 \times \mu \qquad (2)$$

and $$a(5p_{1/2}) = 0.062\ g(I) = 0.062 \times 2 \times \mu \qquad (3)$$

where μ is the nuclear magnetic moment.

For Cd^{111}:

$$a_1(5s) = - 0.4186 \times 2 \times 0.5949 = - 498 \text{ mk} \qquad (4)$$

$$a_1(5p_{1/2}) = - 0.062 \times 2 \times 0.5949 = - 74 \text{ mk} \qquad (5)$$

For Cd^{113}:

$$a_2(5s) = - 0.4186 \times 2 \times 0.6224 = - 521 \text{ mk} \qquad (6)$$

$$a_2(5p_{1/2}) = - 0.062 \times 2 \times 0.6224 = - 77 \text{ mk} \qquad (7)$$

In fig. VI - 3 the expected magnetic hfs in the 5s and $5p_{1/2}$ levels of the odd isotopes are shown. With these data the distances of the

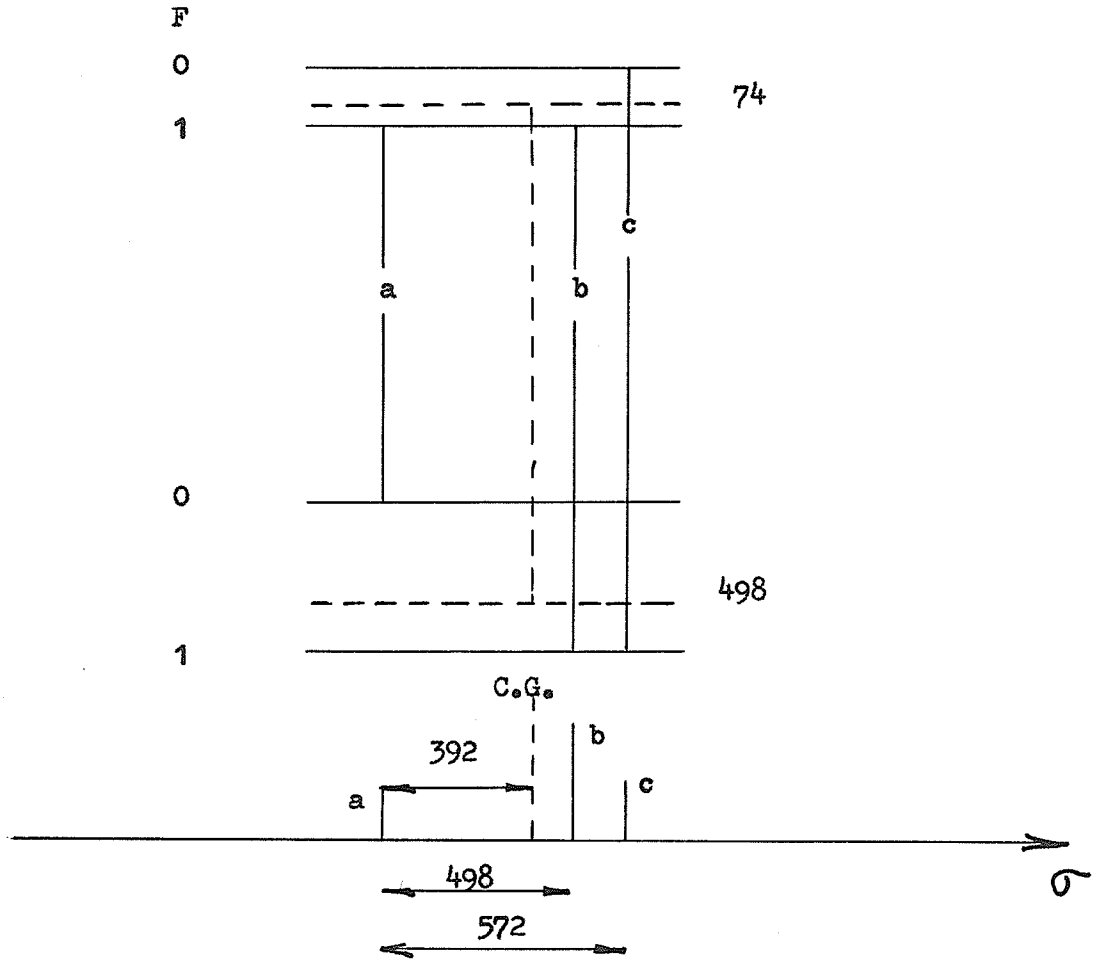

Fig. VI - 3a) Expected magnetic structure of the levels $5p_{1/2}$ and 5s in Cd^{111} II, using the nuclear magnetic moment given by Mack[34]. The relative positions of the components a, b and c, with their center of gravity, are shown. Distances are given in mk.

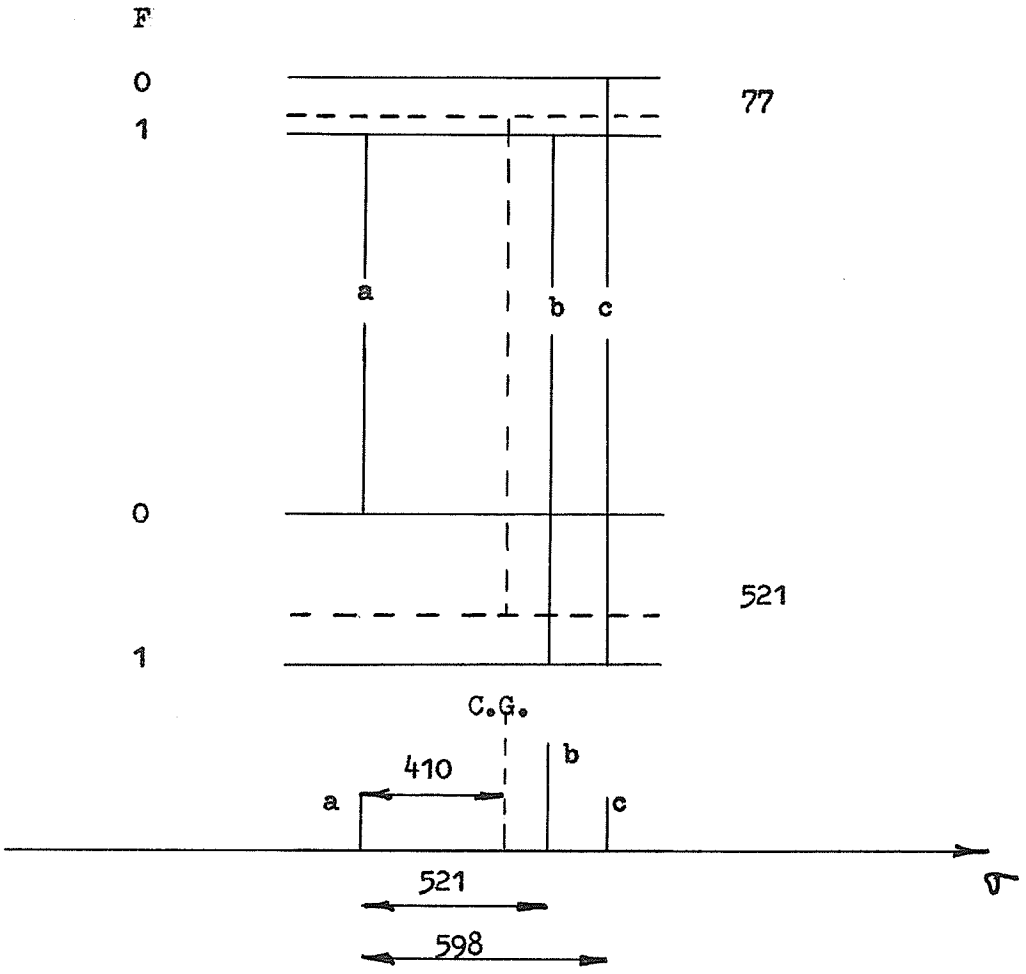

Fig. VI - 3b) Expected magnetic structure of the levels $5p_{1/2}$ and 5s in Cd^{113} II, using the nuclear magnetic moment given by Mack[34]. The relative positions of the components a, b and c, with their center of gravity, are shown. Distances are given in mk.

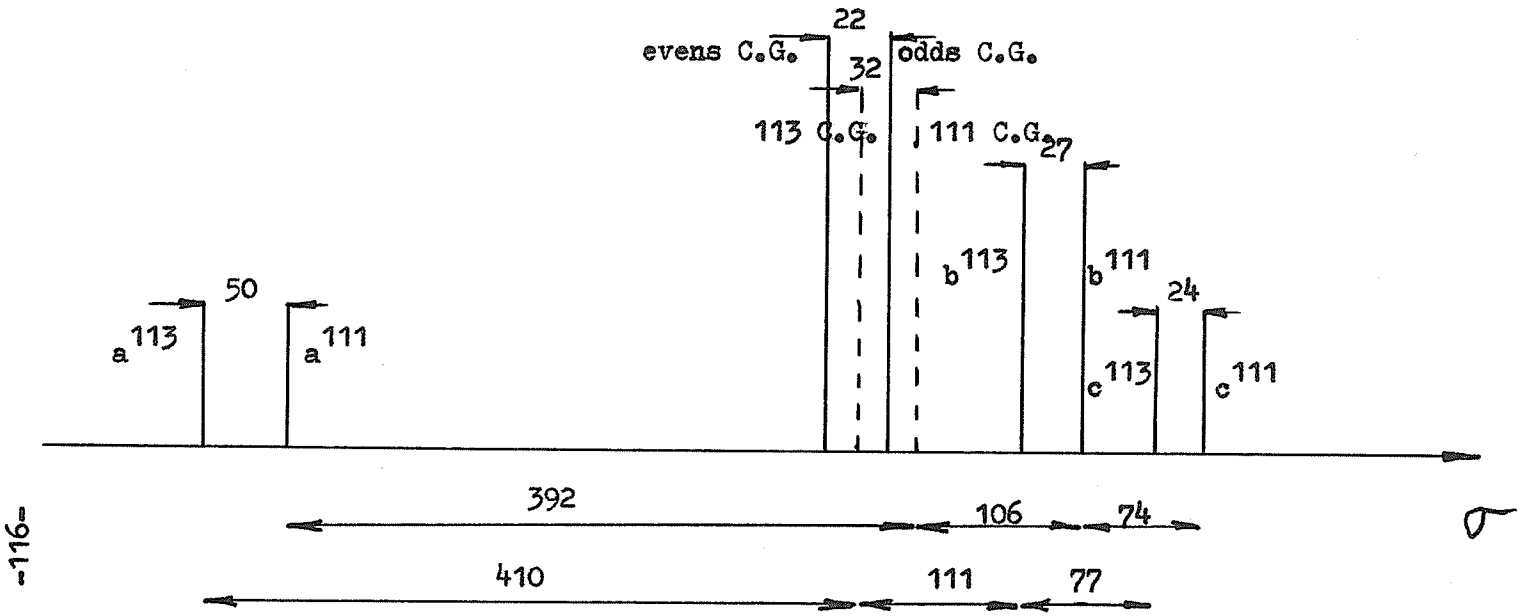

Fig. VI - 4) Calculated distribution of the magnetic components of the odd isotopes and their positions relative to the evens' center of gravity. The distance between the odds' and evens' center of gravity was taken equal to that of Cd I 3261 Å times 1.9. Distances are given in mk units and they, as well as the intensities, are to scale.

various components to their centers of gravity can be computed. Then, using equation (1) it is possible to estimate the distribution of the components due to the odd isotopes. The results of this calculation are shown in fig. VI - 4). When these estimates have been made it is possible to compute the pattern expected when the 2 cm spacer is used. This pattern is shown in fig. VI - 5).

Fig. VI - 1) shows the pattern observed with the 2 cm spacer. Components 2 and 3 in this pattern must be due to the odd isotopes as evidenced by their intensities and by comparison with previous results obtained by Sutherland. Fig. VI - 5) shows the computed pattern, and a comparison of these two figures conclude that the assumptions made above are reasonable. Component 3 of the 2 cm pattern is due to a superposition of component a^{111} and b^{111}. The calculated separation of a^{111} and b^{111} is only 2 mk and it would be impossible to resolve this. Component 2 of the 2 cm pattern arises from a blend of the unresolved components a^{113} and b^{113}. Again, these two components lie so close together that their resolution is not expected. The calculated separation of component 3 of the 2 cm pattern and the center of gravity of the evens is 105 mk while the observed separation is 107 ± 3 mk in good agreement. The calculated separation of component 2 and 3 of the 2 cm pattern is 35 mk while the observed one is $38 \pm$ in satisfactory agreement.

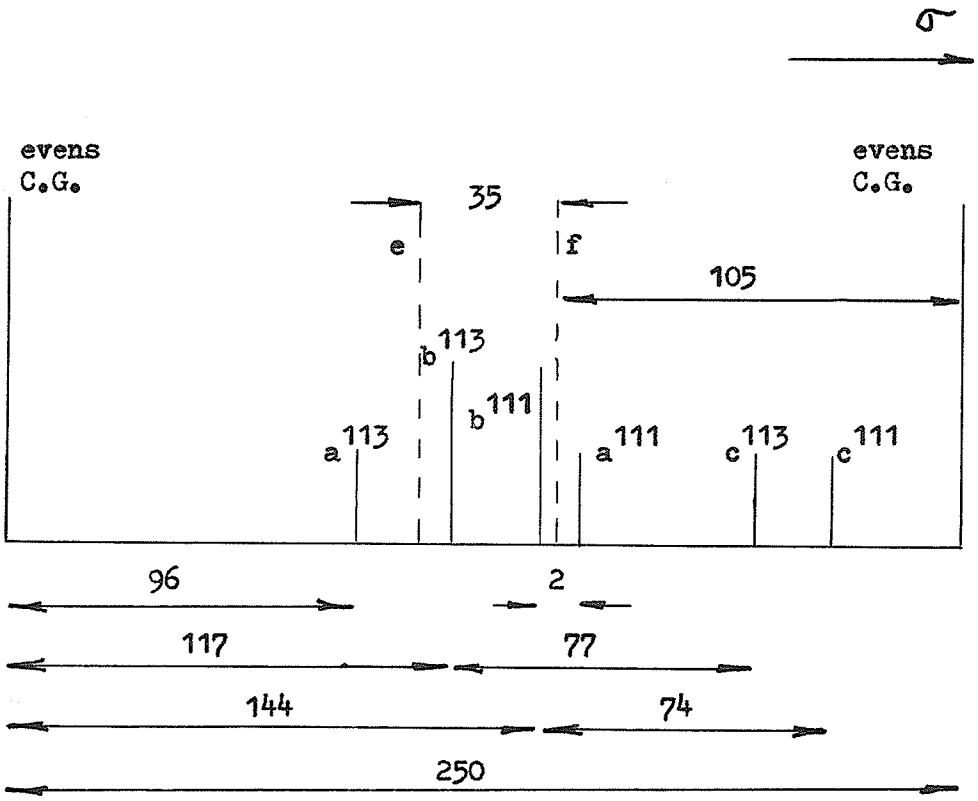

Fig. VI - 5) Schematic drawing of the calculated pattern with the 2 cm spacer. Separations are given in mk. The distribution of the components was taken from fig. VI - 4). Distances and relative intensities are approximately to scale. e stands for the center of gravity of a^{113} and b^{113}, and f stands for the center of gravity of a^{111} and b^{111}.

In order to make corrections to the position of the even isotopes observed with the 5 cm spacer, the distribution of the components due to the odd isotopes in this pattern must be determined by calculation. Fig. VI - 6) is a schematic drawing of the calculated 5 cm pattern. The measured distance between components 1 and 2 of the 5 cm pattern, is the distance between the components produced by the 114 isotope and the m component, which is placed at the center of gravity of components 112, b^{113} and c^{111}. The distance between 112 and m is calculated to be 2 mk. Therefore the isotope shift between components 114 and 112 is 2 mk smaller than the measured separation between components 1 and 2.

With the revised estimate of the isotope shifts between the even isotopes it is now possible to calculate the ratio between these isotope shifts, which are shown in fig. VI - 6), and those in Cd I 3261 Å. This ratio is 1.8 with an accuracy no better than 0.1 and is slightly smaller than the one obtained as a first approximation. This new ratio produces a different distribution of the magnetic hfs components of the odd isotopes, since the distance between the centers of gravity of the odd's and even's components is a bit smaller. For the 2 cm spacer the calculated pattern takes the form shown in fig. VI - 7). However, the separation between the e and f components does not agree very well with the experimental result. The calculated distance is 33 mk

while the measured distance is 38 ± 2 mk. To take this discrepancy into account it must be remembered that, according to Kelly and Tomchuk's data[26], the position of the centers of gravity of the odd components relative to the even ones in Cd I 3261 Å are known with an uncertainty of 1.6 mk for Cd^{111} and 1.3 mk for Cd^{113}. When these uncertainties are multiplied by 1.8 they become 2.9 mk and 2.3 mk respectively. Then, to fit the experimental results with the assumptions shown above, the assumed position of the center of gravity of Cd^{111} in 2265 Å in Cd II is shifted 1 mk towards higher frequencies with respect to the position shown in fig. VI - 4), and, the center of gravity of Cd^{113} is shifted 2 mk towards lower frequencies.

With this correction and the new values for the ratio between the isotope shifts in Cd II 2265 Å and Cd I 3261 Å the position of the magnetic components as well as the even components in the 5 cm pattern is calculated and shown in fig. VI - 8).

To find the 2 cm pattern it is only necessary to shift in fig. VI - 7) the f component 1 mk to the right (higher frequencies) and the e component 2 mk to the left (lower frequencies). Then, the distance between e and f components is 36 mk which compares favorably with the measured value 38 ± 2 mk, and the agreement

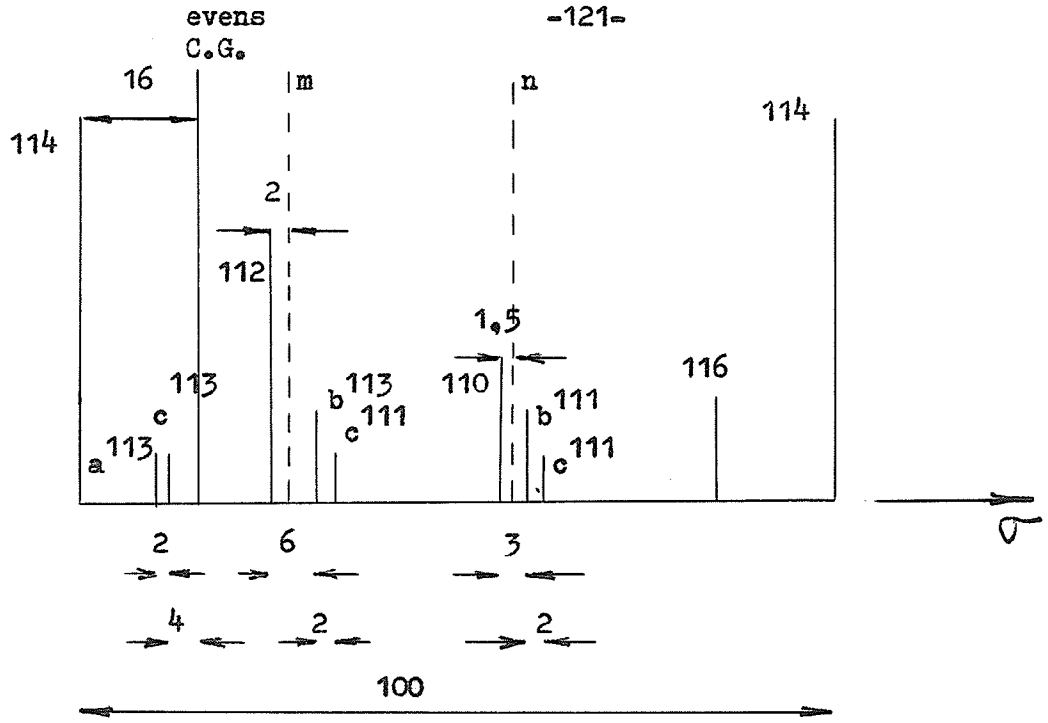

Fig. VI - 6) Schematic drawing showing the position of the odd components relative to the even ones when using the 5 cm spacer and a factor 1.9 to multiply the distances between components of Cd I 3261 Å. In this way it is possible to find an approximate value of the distance between 112 and m components (m stands for the center of gravity of 112, b^{113} and c^{111}) and the distance between 110 and n (n stands for the center of gravity of the components 110, b^{111} and a^{111}). Once these distances are calculated, a second approximation may be obtained considering that the m and n components were the measured ones. With the new separations between even compponents it is possible to calculate a new factor, comparing these values with those of Cd I 3261 A^{o}. A factor of 1.8 is estimated to be a good value for a second approximation. As the components a^{113} and c^{113} lie almost midway between 114 and 112, in this approximation they are neglected.

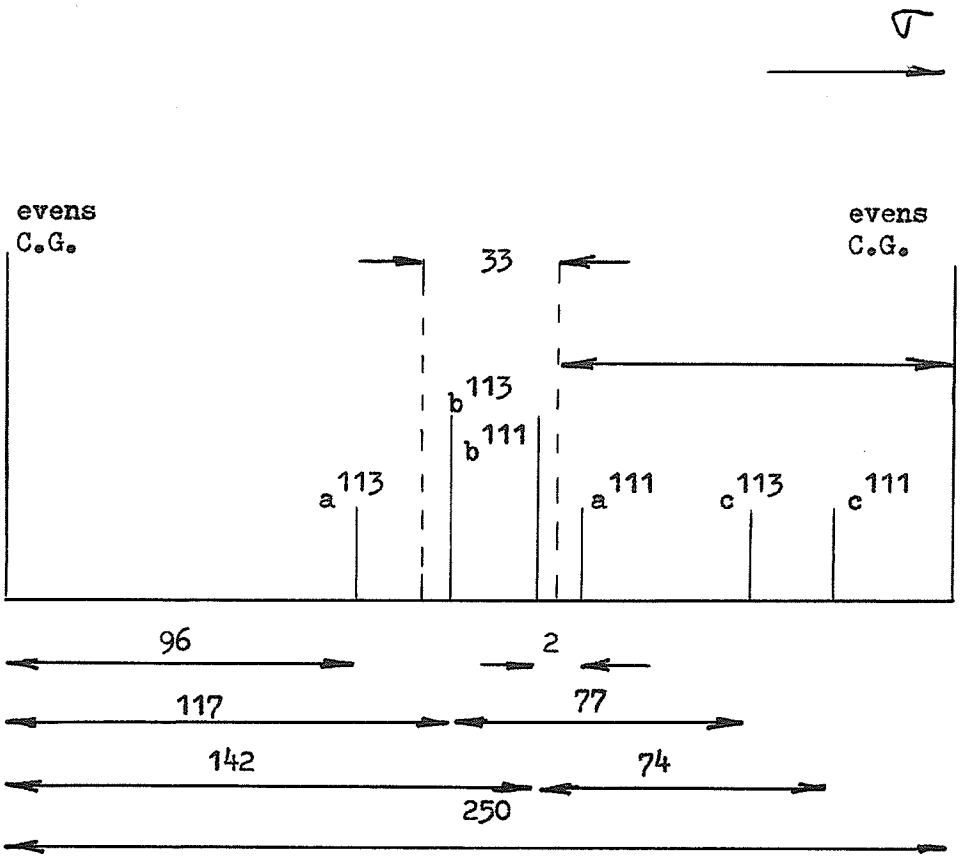

Fig. VI - 7) If the factor is assumed to be 1.8 the expected pattern displayed in fig. VI - 5) takes this form. As before, e stands for the center of gravity of a^{113} and b^{113}, and f stands for the center of gravity of b^{111} and a^{111}. The distance from f to the evens center of gravity agrees with the experimental result. The distance from e to f is a bit too low as compared with the measured value. It is assumed that the center of gravity of 113 should be 2 mk towards lower frequencies than expected, and the center of gravity of 111 should be about 1 mk towards higher frequencies than expected. As pointed out these shifts are within the limits of the values given by Kelly and Tomchuk for Cd I 3261 Å.

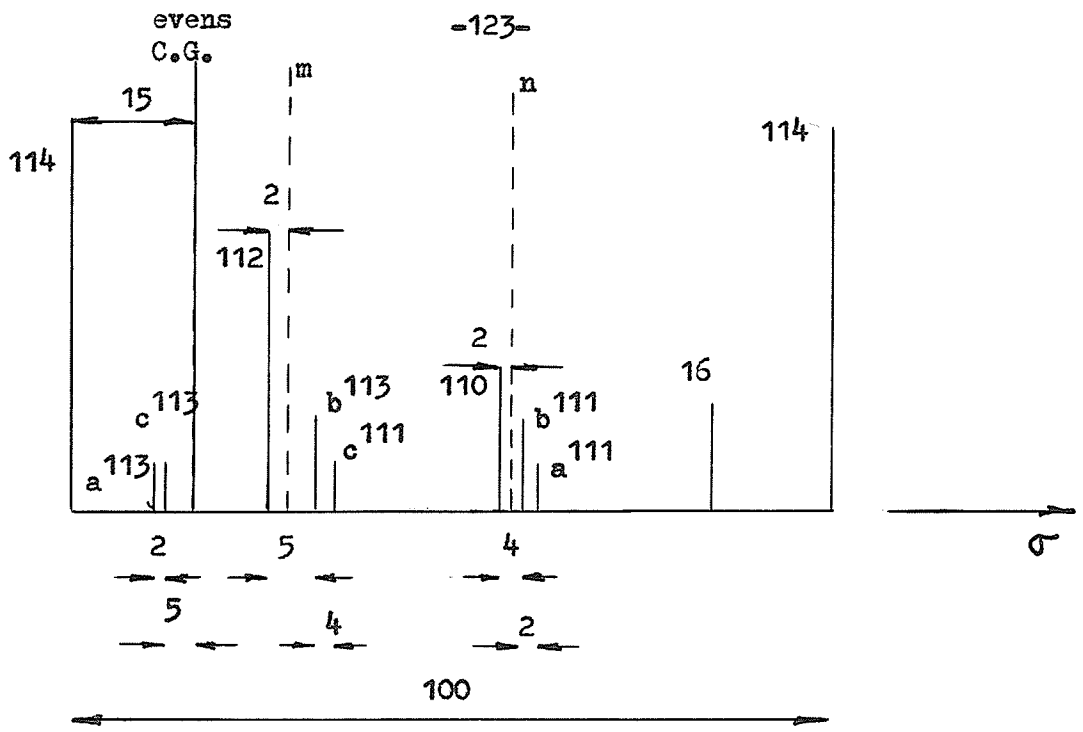

Fig. VI - 8) Assuming the isotope of mass 113 has the center of gravity of its components 2 mk to the low frequency side and the 111 one, 1 mk to the high frequency side, relative to the positions shown in fig. VI - 4), and using a factor 1.8 to multiply the separations of Cd I 3261 Å, this pattern is obtained for the 5 cm spacer. m, as before, stands for the center of gravity of 112, b^{113} and c^{111}, and n stands for the center of gravity of 110, b^{111} and a^{111}. It should be noted that the distances from 114 to m and from m to n, agree within the limits of error with the experimental results. A small correction allowing for the components a^{113} and c^{113} can be made.

between calculated (fig. VI - 8) values and the observed values (fig. VI - 2) is good.

It is also possible to estimate the influence of the a^{113} and c^{113} components in the 5 cm pattern shown in fig. VI - 8). According to the experimental resolving limit, the apparatus half width is estimated to be 9 mk (see chapter V). Then, if these two components are assumed to be placed in their center of gravity with an intensity equal to the sum of their intensities, the profile of this resultant component has half its maximun intensity at the position of the 114 component. The same is true for the 114 component at the position of the center of gravity of a^{113} and c^{113}. When a plot of the profiles of these lines is made it appears that the maximun of the 114 component is shifted in about 0.3 mk towards the components a^{113} and b^{113}. As this value is well inside the limit of the experimental errors, this correction is neglected. The same is valid for the influence of the blend of the components a^{113} and b^{113} on the component 112.

Chapter VII

C O N C L U S I O N S

According to the calculations performed in chapter VI the isotope shift of the transition $5s\ ^2S_{1/2} - 5p\ ^2P_{1/2}$ of six isotopes in Cd II has been observed. They are equal to those of Cd I 3261 Å ($5s^2\ ^1S_0 - 5s5p\ ^3P_1$) times $1.8 \pm .1$. This factor is a bit larger than the one in mercury given by Kopfermann[29]. However, the 1.6 factor in mercury refers to the isotope shifts of the ground states of Hg I and Hg II, while here the 1.8 factor connects the isotope shifts of the transitions 3261 Å in Cd I and 2265 Å in Cd II, and not the splittings of their ground states.

In fig. VII - 1) the observed isotope shifts are shown. The components produced by the isotopes 108 and 106 could not be observed due to the low natural relative abundance of these isotopes. The relative position of the odd components was based on the assumption that the magnetic splitting of the terms 5S and $5P_{1/2}$ follow, respectively, formulas 3.5 and 3.6 of Sutherland's thesis[47] (equations (1) and (2) of chapter I, provided equation (1) is multiplied by the Fermi-Segrè factor, computed according to the method shown by Crawford and Schawlow[10]), which only include the Fermi-Segre factor and the relativistic corrections called $F_r(J,Z)$ and $H_r(L,Z)$ in chapter II (they were called $K(J,Z)$ and $\lambda(L,Z)$, respectively, in chapter I), but do not include any

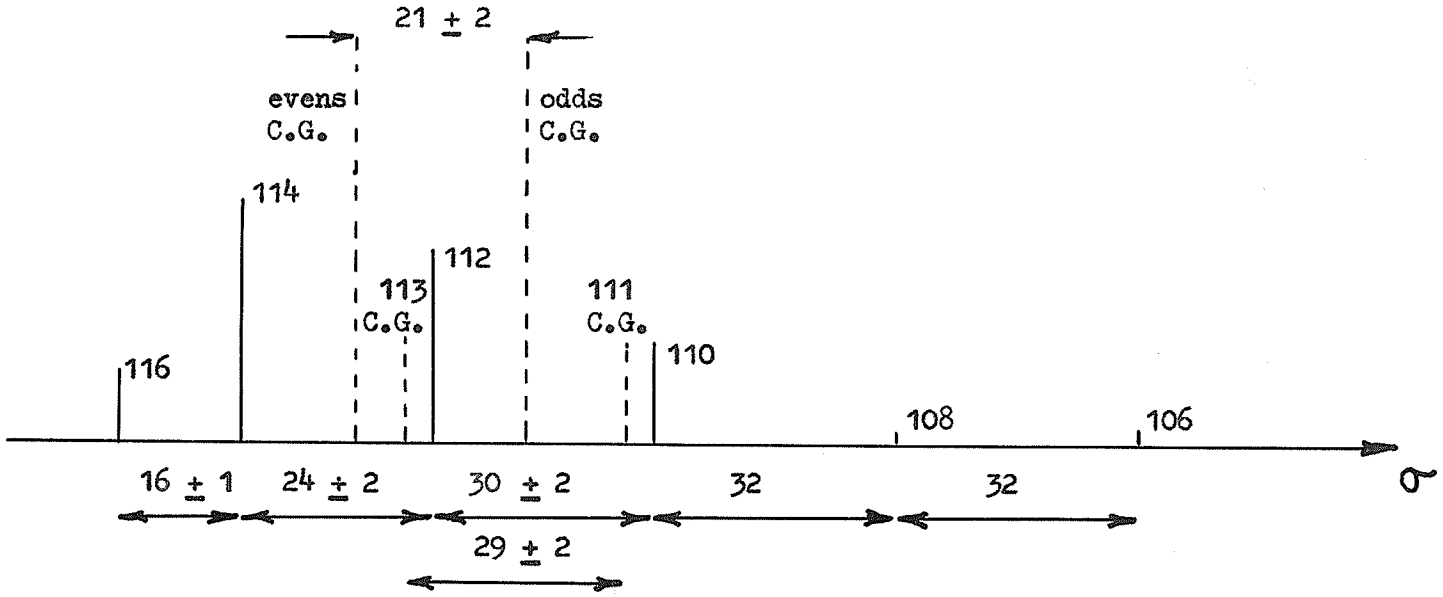

Fig. VII - 1) Isotope shifts in the transition 2265 Å ($5s\ ^2S_{1/2} - 5p\ ^2P_{1/2}$) of Cd II. As the components 108 and 106 were too weak they were not observed. The values quoted here for the separations of those components were found from the isotope shifts in Cd I 3261 Å, times 1.8. Distances are given in mk. The separation between the odds and evens center of gravity agrees with that found re-interpreting Suhterland's data (see chapter I).

correction to take into account the finite volume of the nucleus through which the charge and magnetic moment are spread.

A summary of the measured isotope shifts in Cd II 2265 Å is given in table VII - 1. These values are compared with other isotope shifts previously measured in different cadmium lines. This comparison is shown in table VII - 2.

TABLE VII - 1

Observed isotope shifts in Cd II 2265 Å.

Isotope pair	114, 116	112,114	110,112	111, 113
Isotope shift (mk)	16 ± 1	24 ± 2	30 ± 2	29 ± 2

TABLE VII - 2

Comparison of the isotope shifts found in Cd II 2265 Å with others previously reported in different cadmium lines.

Cd line	Reference number	114, 116	112, 114	110, 112	111, 113
2265	present work	16 ± 1	24 ± 2	30 ± 2	29 ± 2
2288	(27)	-	17.0 ± 0.6	13.2 ± 1.0	-
3261	(26)	9.3 ± 0.3	13.5 ± 0.4	16.3 ± 0.5	17 ± 3
4416	(31)	34.7 ± 0.8	48.8 ± 0.6	52.0 ± 0.4	54.1 ± 3.4

Kelly and Tomchuk[26] have found the relative shifts between the various isotopes taking the shift between components 110 and 112 equal to one. Analogous calculations were made before by Kuhn and Ramsden[31] with the isotope shifts in Cd II 4416 Å. To find similar ratios between the isotope shifts found in Cd II 2265 Å it is necessary to adjust the isotope shifts shown in table VII - 1 for the normal mass effect. Within the limits of experimental errors, the normal mass effects between any two isotopes may be taken as 4 mk. This effect has opposite sign than the volume effect. Then to find the isotope shifts produced by the volume effect, 4 mk must be added to the values shown in table VII - 1. The specific mass effect is assumed to be small.

TABLE VII - 3

Comparison of the relative shifts due to the volume effect found in different works. The separation between components 110 and 112 is taken equal to 1.00. The percentage errors of the ratios found in the present work, are: 10 % for the isotope pair 116, 114; 12 % for 114, 112; and 11 % for the 111, 113 pair.

Isotope pair	present work	Kelly and Tomchuk	Kuhn and Ramsden
½(106, 110)	-	1.07	1.04
108, 110	-	-	1.00
110, 112	1.00	1.00	1.00
111, 113	0.97	1.03	1.03
112, 114	0.83	0.85	0.93
114, 116	0.59	0.62	0.65

The ratios found for the relative isotope shifts in the present work are somewhat lower than the previously reported shifts in other works. The large uncertainties in the present work do not permit to obtain a definite answer to the discrepancy found for the relative isotope shift in the pair 112, 114 by Kelly and Tomchuk with the value reported by Kuhn and Ramsden for the same pair of isotopes.

Kuhn and Ramsden[31] have plotted the relative isotope shifts in Cd II 4416 Å versus the neutron number for the various natural isotopes of cadmium. This plot has displayed a "jump" in the isotope shifts when N = 66, that is to say, in the isotope shift between 112 and 114. In the same graph these authors have plotted the same relative isotope shifts in tin. Both curves show the same downward trend when the neutron number is increasing, and the same "jump" when N = 66. The same relative isotope shifts for the same neutron numbers in different elements were found previously in Nd, Sm and Gd (see references in Kuhn and Ramsden's paper). This seems to indicate that to add a pair of neutrons to a nucleus often has the same effect on the nuclear charge distribution in nuclei whose atomic numbers differ in two.

As it was pointed out in chapter II - b - 2), the changes of the isotope shift in terms of the neutron number are imputed to nuclear

deformation. The deformation is described by the parameter which is connected to the quadrupole moment. The isotope shift is proportional to $\Delta N \times \frac{\partial(\beta^2)}{\partial N}$ (see equation (18), chapter II - b - 2). The change in the isotope shift from one isotope pair to the next one, is proportional to the second derivative $\frac{\partial^2(\beta^2)}{\partial N^2}$. Therefore the trend shown by the curve of the relative isotope shifts plotted against the neutron number by Kuhn and Ramsden[31], indicates that the second derivative $\frac{\partial^2(\beta^2)}{\partial N^2}$ is negative. Then, it would be expected that β^2 as a function of N is approaching a maximun in the range covered by N in the natural isotopes of cadmium, probably between N = 65 to N = 70, as compared by Kuhn and Ramsden with other nuclei with $I > \frac{1}{2}$ and therefore, nuclei where the deformation parameter may be calculated from direct measure of the quadrupole moment.

Regarding to the "jump" found when N = 66, Kuhn and Ramsden suggest that it can be due to the completion of sub-shells, since N = 66 has 16 neutrons less than the magic number 82, and the levels $4d_{3/2}$ and $6h_{11/2}$ need respectively 4 and 12 neutrons to be filled. The sequence of these nuclear levels is found with the shell model and agrees with the model used by Nilsson (see reference in Kuhn and Ramsden's paper). However, these authors consider the assumption that the "jump" is produced when these levels start being filled, is rather hypothetical and that it is necessary to obtain more experimental data to confirm it.

As reported in other cadmium lines, the odd-even stagerring found in Cd II 2265 Å is also very pronounced. The staggering effect is now ascribed to a tendency of nuclei with odd neutron number to be less deformed than those with an even neutron number.

A C K N O W L E D G E M E N T S

The author wishes to express his sincere thanks to Professor F.M. Kelly, under whose advise and direction this experimental work was performed.

He also is very grateful to Mr. L.O. Dickie for valuable help concerning the experimental work, and to Dr. E. Tomchuk for interesting discussions and ideas.

BIBLIOGRAPHY

1. Bacher, R. and Goudsmit, S.; Atomic Energy States, McGraw-Hill Books Company, New York (1932).

2. Bartlett, J. H.; Nature 128, 408, (1931).

3. Born, M. and Wolf, E.; Principles of Optics, Pergamon Press, New York, (1959).

4. Breit, G.; Theory of Isotope Shift, Rev. Mod. Phys. 30 # 2, 507, (1958).

5. Breit, G.; Phys. Rev., 42, 348, (1932).

6. Burridge, J. C., Kuhn, H. and Pery, A.; Proc. Phys. Soc. 66B, 963, (1953).

7. Casimir, H. B. G.; On the Interaction Between Atomic Nuclei and Electrons, W. H. Freeman and Co., San Francisco, (1963).

8. Condon, E. U. and Shortley, G. H.; The Theory of Atomic Spectra, Cambridge University Press, (1964).

9. Condon, E. U.; Phys. Rev. 36, 1121, (1930).

10. Crawford, M. F. and Schawlow, A. L.; Phys. Rev. 76, 1310, (1949).

11. Crawford, M. F. et al.; Can. J. Phys., A28, 138, (1950).

12. Davydov, A. S.; Quantum Mechanics, Pergamon Press, New York,(1965).

13. Dickie, L.O.; Ms. of Sci. degree Thesis, University of Otago, New Zealand, (1967).

14. Dirac, P. A. M.; The Principles of Quantum Mechanics, Oxford University Press, (1958).

15. Fermi, E. and Segrè, E.; On the Theory of Hfs, Memotie dell' Accademia d'Italia (Fisica), 131, (1933),(translated by Sykes).

16. Goudsmit, S.; Theory of Hyperfine Structure Separations, Phys. Rev., 37, # 6, 663, (1931).

17. Goudsmit, S. and Bacher, R. F.; Phys. Rev., 34, 1501, (1929).

18. Goudsmit, S.; Phys. Rev., 43, 636, (1933).

19. Herzberg, G.; Atomic Spectra and Atomic Structure, Dover Publications, New York, (1944).

20. Hindsmarsh, W. R.; Atomic Spectra, Pergamon Press, (1967).

21. Hughes, D.S. and Eckart, C.; Phys. Rev. 36, 694, (1930).

22. Jackson, J. D.; Classical Electrodynamics, John Wiley and Sons, Inc., New York, (1967).

23. Jacquinot, P.; Reps. on Prog. Phys. 23, 267, (1960).

24. Jones, E. G.; Proc. Phys. Soc. of London, 45, 625, (1933).

25. Kelly, F. M.; Determination of Nuclear Spins and Magnetic Moments by Spectroscopic Methods, Handbuch der Physik, 37/1, 59, (1958).

26. Kelly, F. M. and Tomchuk, E.; Isotope Shift in Cd I. Intercombination Resonance Line 3261 Å, Proc. Phys. Soc. 24, 689, (1959).

27. Kelly, F. M. and Tomchuk, E.; Isotope Shift in the Resonance Line 2288 Å of Cd I; Proc. Phys. Soc. 28, 1304, (1961).

28. Kelly, F. M. and Sutherland, J. B.; Cand J. Phys. 34, 521,(1956).

29. Kopfermann, H.; Nuclear Moments, Academic Press, Inc., New York (1958).

31. Kuhn, H. G. and Ramsden, S. A.; Proc. Roy. Soc., A237, 485, (1956).

32. Leland, W. and Nier, A.; Phys. Rev., 73, 1206, (1948).

33. Lorentz, H. A.; The Theory of Electrons, B.G. Teubner, (Leipzig), (1909).

34. Mack, J. E.; Rev. of Mod. Phys., 22, 64, (1950).

35. Meissner, K. W.; Interference Spectroscopy, Parts I and II, J.O.S.A., 31, # 6, 405, (1941) and 32, # 4, 185, (1942).

36. Messiah, A.; Quantum Mechanics, John Wiley and Sons, Inc., New York, (1966).

37. Moore, Ch. E.; Atomic Energy Levels, Nat. Bur. Stand., Circular 467, Washington, (1962).

38. Pauling, L. and Goudsmit, S.; The Structure of Line Spectra, McGraw-Hill Book Company, Inc., New York, (1930).

39. Proctor, W. G. and Yu, F. C.; Phys. Rev., 76, 1728, (1949).

40. Racah, G.; Isotope Displacement in Hfs; Nature, 129, 723, (1932).

41. Rosenthal, J. E. and Breit, G.; Phys. Rev. 41, 459, (1932).

42. Ruark and Urey, H.; Atoms Molecules and Quanta, Dover Publications, New York, (1964).

43. Slater, J. C., Phys. Rev., 34, 1293, (1929).

44. Stacey, D. N.; Isotope Shifts and Nuclear Charge Distributions, Reps. Prog. Phys., 29, Part I, 171, (1966).

45. Stone, J.; Radiation and Optics, McGraw-Hill Book Company, Inc. (1963).

46. Strominger, D., Hollander, J. M. and Seaborg, G. T.; Rev. of Mod. Phys., 30, 585, (1958).

47. Sutherland, J. B.; Ms. of Sci. degree Thesis, University of Manitoba, (1957).

48. Svensson, K. F.; Measurements of the Dispersion of Air for Wavelengths from 2302 to 6907 Å, Arkiv Fysik, band 16 nr 35,(1960).

49. Tolansky, S.; High Resolution Spectroscopy, Methuen and Co., London, (1947).

50. Tomchuk, E.; Optical Hfs Structure Studies in Cd and Ba., PhD degree Thesis, University of Manitoba, (1964).

51. Trees, R. E.; Hfs Formulas for LS Coupling, Phys. Rev., 92, # 2, 308, (1953).

52. Weiskopf, V and Wigner, E.; Calculation of the Natural Line Width on the Basis of Dirac's Theory of Light; Zeits. fur Physik, 63, 54, (1930), (translated by Sykes, J. B.).

53. Weisskopf, V.; The Width of Spectral Lines in Gses, Physikalische Zeits., 34, 1, (1933), (translated by the United States Atomic Energy Commission).

54. White, H. E., Introduction to Atomic Spectra, McGraw-Hill Book Company, Inc., (1934).